The speed controlled leakhole (SCL)

THE SPEED CONTROLLED LEAKHOLE (SCL)

W. de VAAN

May 1984 R 669 D

CONSULTANCY SERVICES | P.O. BOX 85
WIND ENERGY | 3800 AB AMERSFOORT
DEVELOPING COUNTRIES | THE NETHERLANDS

WIND ENERGY GROUP

Technical University Eindhoven
Faculty of Physics
Laboratory of Fluid Dynamics and Heat Transfer
P.O. Box 513, 5600 MB Eindhoven, the Netherlands

CONTENTS page

SYMBOLS

A_p	= area of piston	(m^2)
b	= thickness of SCL-valve	(m)
C	= coefficient	(kg m^{-1})
D	= diameter supply feeder	(m)
dp	= diameter piston	(m)
F	= pump rod force	(N)
Fst	= steady drag force	(N)
g	= acceleration of gravity	(m s^{-2})
H	= lifting head	(m)
h	= gap height between valve and seat	(m)
m_v	= mass of SCL-valve	(kg)
n	= rotational speed	(s^{-1})
Q	= torque	(N m)
$\overline{Q}$	= average torque	(N m)
Q_p	= torque demanded by pump	(N m)
Q_r	= rotor torque	(N m)
R	= radius	(m)
r	= radius SCL-valve	(m)
s	= stroke of pump	(m)
t	= time	(s)
V_p	= velocity piston	(m s^{-1})
V_o	= velocity piston when SCL closes	(m s^{-1})
V_w	= velocity wind	(m s^{-1})
α	= crank-angle with regard to lowest position	
α_{cl}	= valve closure angle	
α_1	= angle when SCL-valve leaves valve stop	
α_{scl}	= angle when SCL-valve closes	
ω	= angular velocity	(rad s^{-1})
ρ_w	= density water	(kg m^{-3})
Φ	= flow	(m^3 s^{-1})
Φ_{close}	= flow when SCL closes	(m^3 s^{-1})
η	= dynamic viscosity	(kg m^{-1} s^{-1})

η_{vol} = volumetric efficiency

η_{mech} = mechanical efficiency

∇_v = volume valve (m^3)

π = 3,14159

λ = tip speed ratio

1. SUMMARY

Within the Consultancy Services Wind Energy Developing Countries (CWD) research has been done on water pumping windmills for developing countries. But coupling a windmill and a pump is not so easy. One of the problems is the relative high starting torque compared with the average torque demanded by the pump. This report describes the efforts to design a system to improve the starting behaviour of the CWD 145 pump in case of coupling on the CWD 2740 windmill.

Chapters 2 and 3 give a more detailed description of the problem and some possible solutions.

Chapter 4 describes the theoretical behaviour of the speed controlled leakhole (SCL).

Chapter 5 describes the first effort to design a SCL and the test results of this SCL I.

On account of these results several times the system has been improved and tested again, which resulted in a final test described in chapter 9. In the discussion in chapter 10 arguments are given why it is necessary to continue the research on this subject, since still some problems are to be solved.

On the other hand we can conclude that some progress is made in improving the starting behaviour of the pump,

- since the starting torque of the pump can be decreased considerably
- and since it is possible to control this starting provision.

2. INTRODUCTION

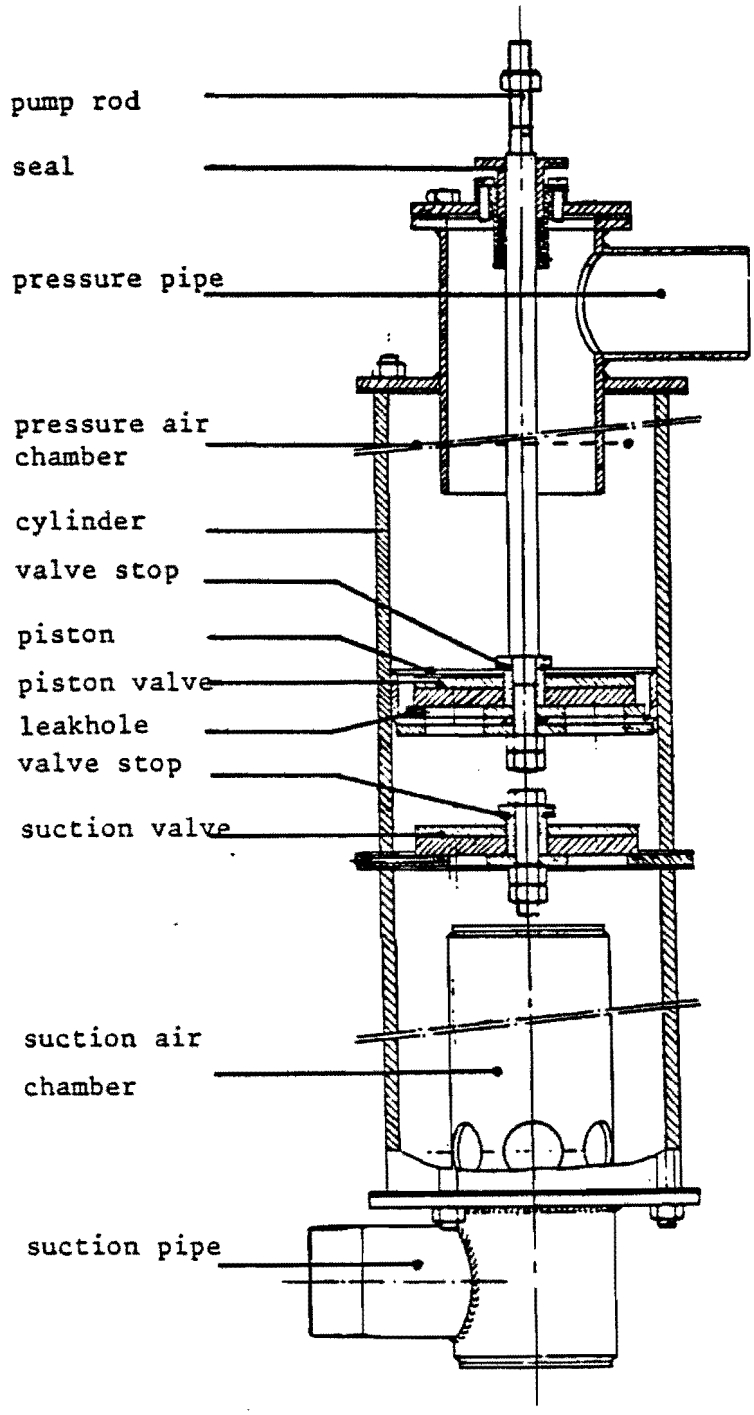

Fig. 2.1. CWD 145 Pump

The CWD develops waterpumping windmills intended for local production in developing countries. For reasons of efficiency and ease of manufacture, the applied pumps are single acting

piston pumps. While a rotor has a quadratic torque-rpm characteristic, the average torque demanded by a single acting piston pump is constant, with the pump torque varying from zero to π times the average pump torque during one cycle. This implies that in principle there is a starting and matching problem:

- a matching problem because of coupling the rotor with a quadratic torque characteristic to a pump with constant average torque. This implies that there will only be one rpm at which the system will run at maximum overall efficiency. The corresponding wind speed is called the design wind speed of the wind pump
- a starting problem because when starting, the rotor has to exceed the peak torque of the pump being π times the average torque. To improve starting behaviour of the wind pump either the starting torque of the rotor can be increased or the peak torque of the pump (when starting) can be reduced. Increasing the starting torque of the rotor requires high solidity slow running rotors that are economically less attractive than rotors with lower solidity. Remember American type windmills, that can be characterised as being multi (12 - 48) bladed and with a tip speed ratio of approximately $\lambda = 1$. The windmills as developed by CWD have less blades (6 - 8) and a tip speed ratio of $\lambda = 2$. As a consequence the starting torque is less. So starting behaviour has to be improved by applying starting gadgets, such as a leakhole in the piston. (See lit. I page 154)

However a disadvantage of a leakhole is the reduction of volumetric efficiency of the system.
It is expected that with a controlled flow through the leakhole starting behaviour and volumetric efficiency can be improved:

- at low rpm the flow through the leakhole can be larger than in case of conventional leakhole, hence facilitating starting

- at high rpm the leakhole can be closed, thereby reducing the loss in volumetric efficiency.

The provision to control the flow through the leakhole is called speed controlled leakhole (SCL). The pump on which the SCL is tested is the CWD 145 pump (see fig. 2.1.)

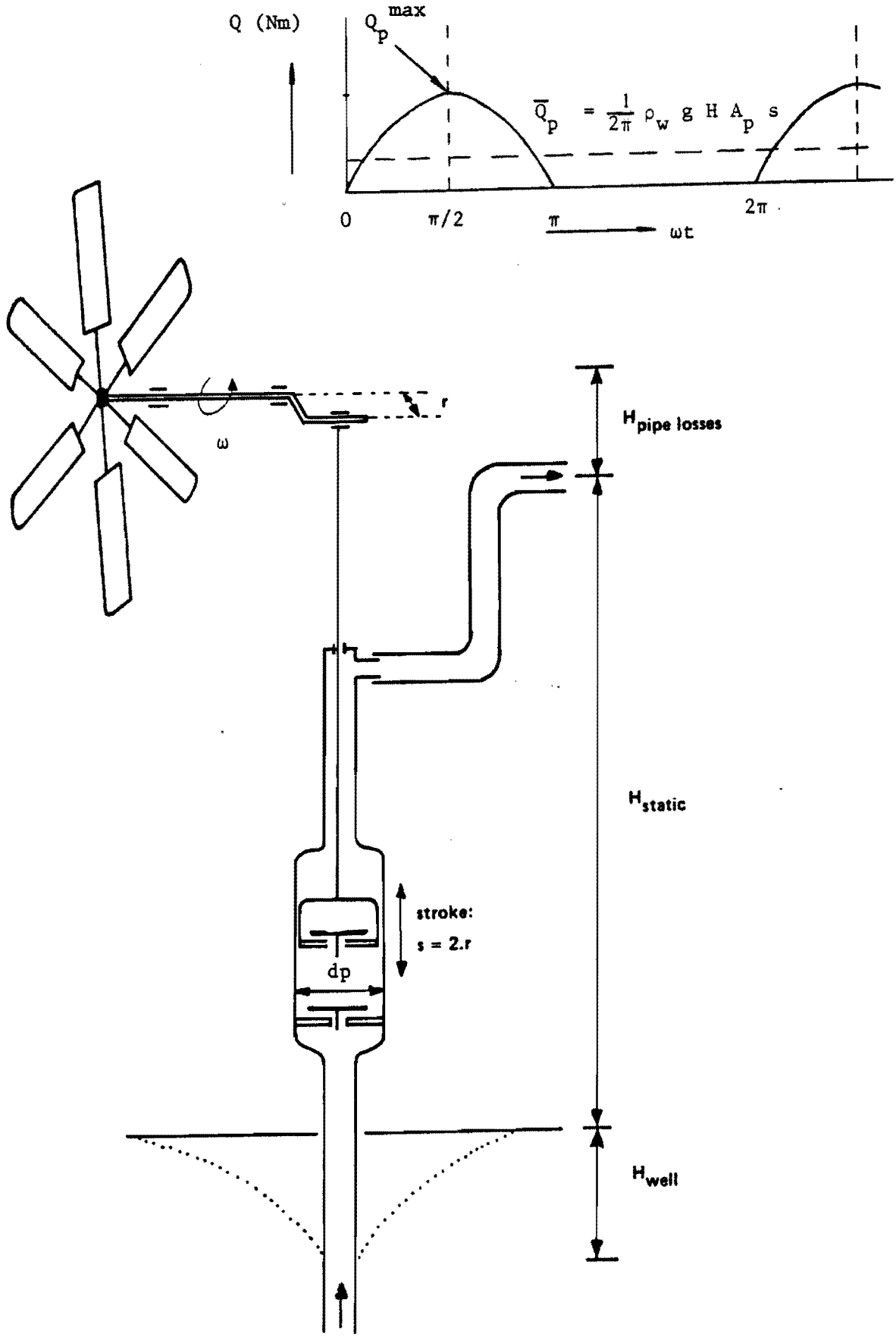

Fig. 3.1. Schematic drawing of a reciprocating piston pump connected to a wind rotor

3. Starting behaviour of a windmill coupled to a single acting piston pump

A piston pump coupled to a rotor by means of a crank/connecting rod mechanism has a torque Q which is sinusoidal during the upward stroke and zero during the downward stroke of the pump (see fig. 3.1.). In order to start without any starting gadget the rotor torque has to exceed the maximum torque of the pump. Once running, the rotor is able to store kinetic energy during the unloaded downward stroke of the cycle, which energy is given to the pump in the loaded upward stroke. This implies that the rotor torque can be equal to the average torque ($\overline{Q}_p$) of the pump.

In Lit. I page 103 the maximum torque $Q_{p,max}$ of the pump has been calculated to be π times the average torque $\overline{Q}_p$. The calculated constant $\overline{Q}_p$ in fact is the ideal average pump torque $\overline{Q}_{p,\,ideal}$.

Since in practice the system has some hydraulic and mechanical friction the real average pump torque will increase for increasing rpm.

In fig. 3.2. the torque-rpm curves for the CWD 2740 rotor for various wind speeds and the torque-rpm curve for a single acting piston pump are given.

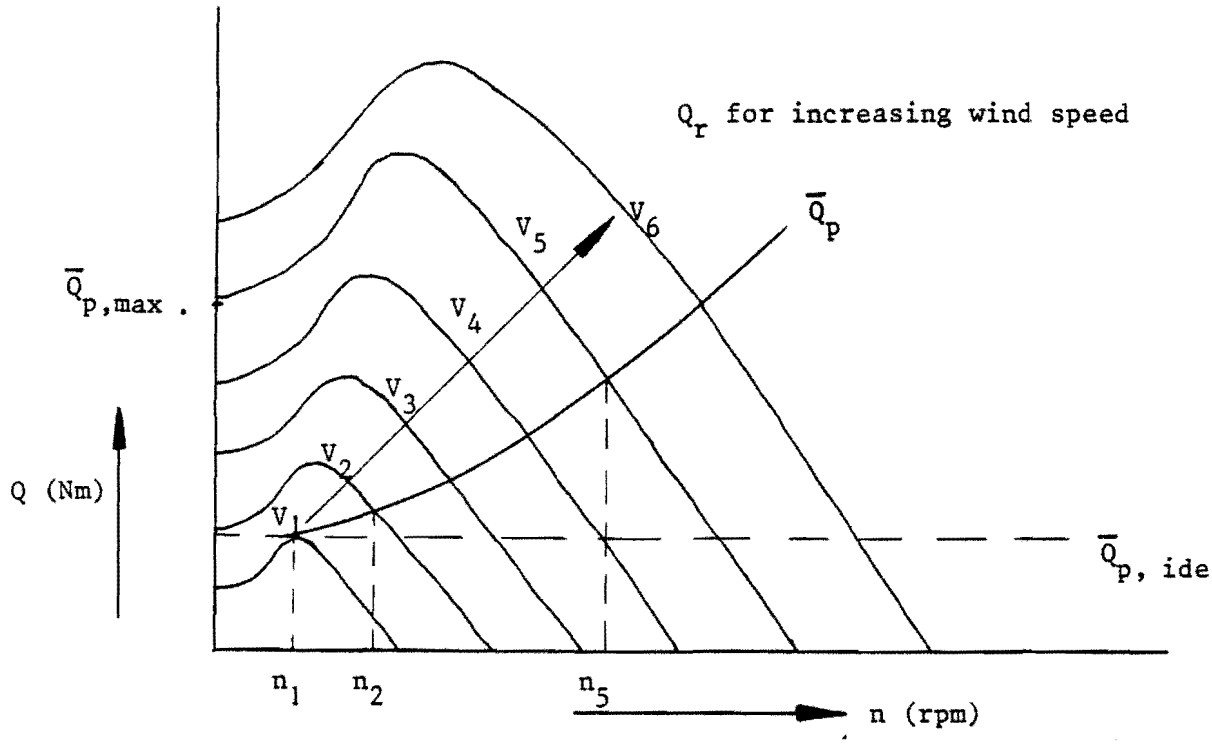

Fig. 3.2. Torque-rpm curves for pump and rotor

Without a starting gadget the rotor torque has to exceed the maximum pump torque $Q_{p,\ max.}$, which is the case for a wind speed $V = V_5$ and a rpm of $n = n_5$. Once running a decreasing wind speed will cause a rpm reduction, but the wind pump will keep on running untill a wind speed of $V = V_1$ (see fig. 3.2.).

The effect of a leakhole - a small hole drilled through the piston - is to reduce the pressure difference over the piston at low piston speeds (= low rpm) and to enable the piston to move to the Top Dead Center (TDC). From the TDC the piston moves unloaded downwards and the rotor can accelerate and store kinetic energy, which energy can be given to the pump during the next upward stroke.
Assuming that in this case the starting torque of the rotor only has to exceed the average pump torque $\overline{Q}_p$ the rotor will

start at a wind speed V_2 (see fig. 3.2.). Hence compared with a pump without a starting gadget the rotor will start at a considerably lower wind speed, improving the so-called availability of the wind pump. A disadvantage of a leakhole however is, that there is a certain amount of leak, which reduces the volumetric efficiency. (See Lit. I page 160)
The volumetric efficiency of the pump can be improved when the leakhole is closed above a certain rpm. This implies that information on the rpm will have to control a valve closing the leakhole.
In practice this will require a more or less sophisticated measurement and control system, which is beyond the scope of a design for developing countries.
A more simple solution is to control the valve by the speed of the piston, considering that the piston speed is proportional to the rpm.

4.1. The development of the SCL

As mentioned in chapter 3, coupling a windmill and a single acting piston pump needs a starting gadget to reduce the starting torque. Until now the CWD uses a small leakhole in the piston to reduce the starting torque.
M. Jacobs in his report of June 1983 (Lit. 2) describes his efforts to develop a mechanism to control the leak through the leakhole. The system evolved from a bypass between suction and pressure side of the pump with a freely moving valve, to a selfregulating leakhole integrated within the design of the piston. (See fig. 4.1.)

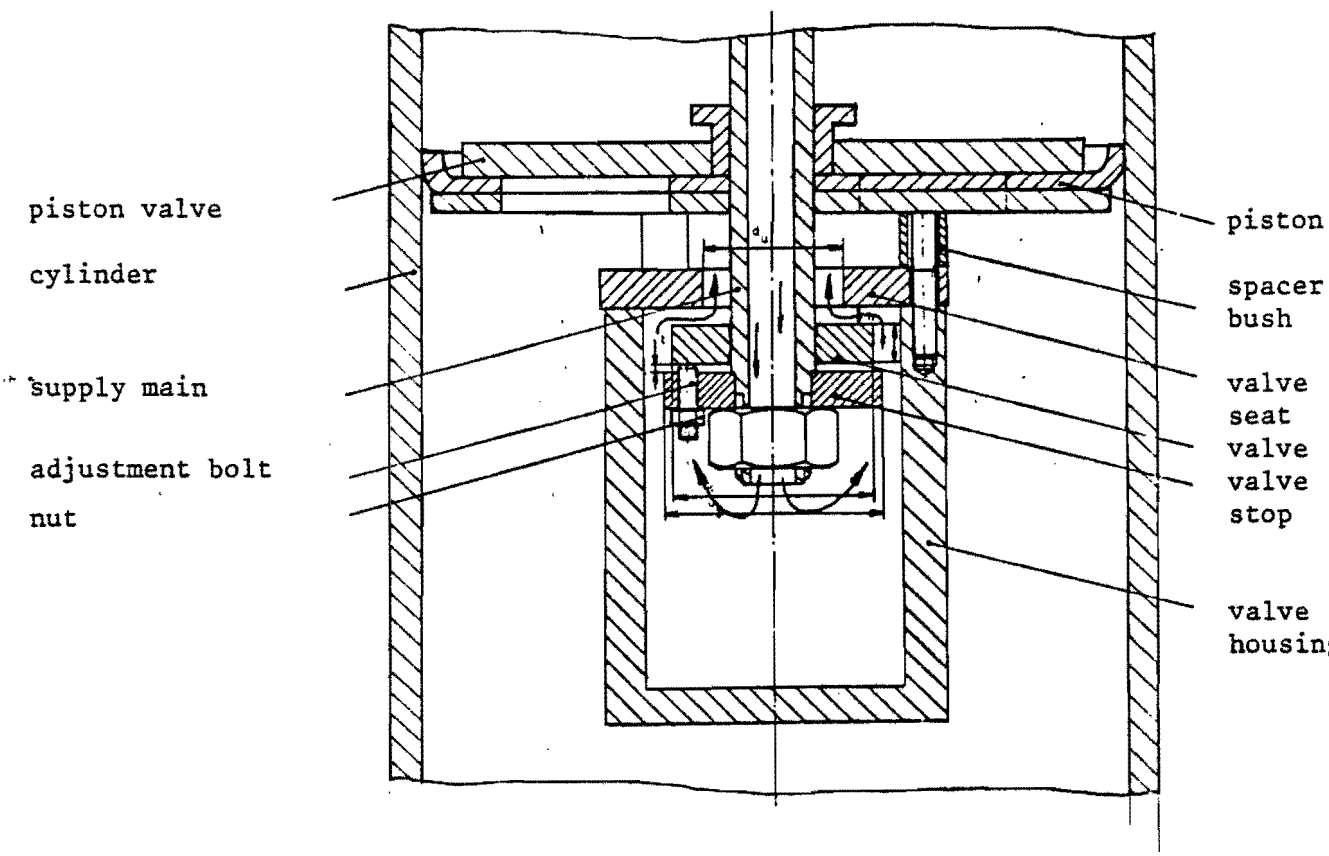

Fig. 4.1. The selfregulating leakhole system of M. Jacobs

The functioning is as follows. The water flows through the supply main into the valve housing. From there the only way out is through the valve system. When the velocity of the water through the valve system is sufficiently high the valve will close. M. Jacobs used a simple model to calculate the flow for which the valve would close, which appeared not to be in accordance with measurements. Specially for the thinner valves the measurements vary considerably from the theory. For this reason it was decided to use the measurements instead of the calculations to develop the SCL-system. Notice however, that M. Jacobs used rather thick valves, which is unrealistic in view of the heavy construction that would be developed in that case. Still it is reasonable that his measurements give use an indication of the dimensions of the SCL.

4.2. The theoretical operation of the SCL

As mentioned in chapter 3 the SCL is meant to be a construction to control the valve of a leakhole by the speed of the piston. If for instance the leakhole could be closed at a piston speed corresponding with the rpm of $n = n_1$ in fig. 3.2., the windmill-pump combination could start pumping at a wind speed of $V_w = V_1$, since in this case for lower rpm than n_1 the rotor torque exceeds the pump torque. However the piston speed V_p is sinusoidal and increasing for increasing rpm. (See fig. 4.2.).

$$V_p = \tfrac{1}{2} s \omega \sin \omega t$$

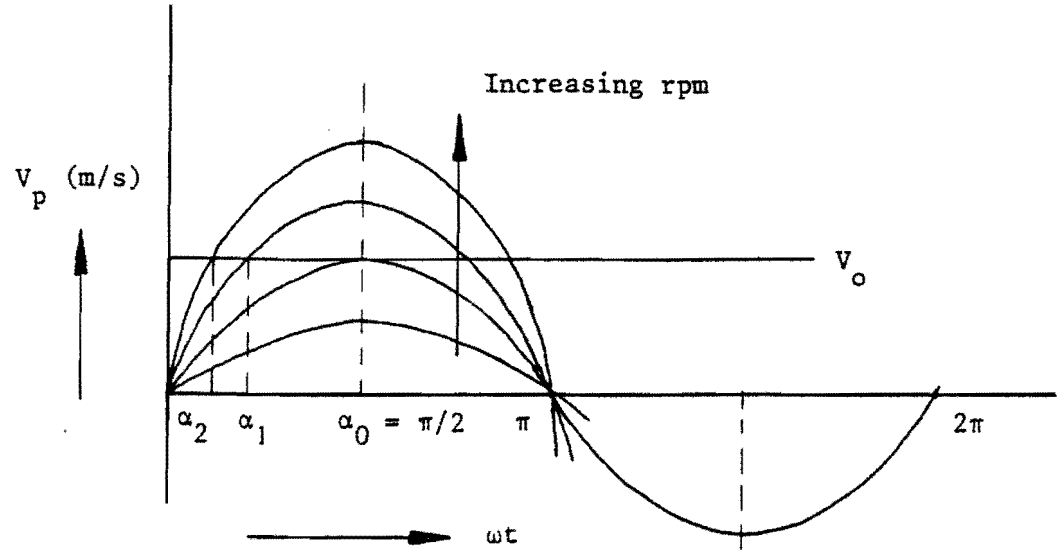

Fig. 4.2. The piston speed V_p for increasing rpm

This implies that V_p is maximal for $\omega t = \alpha_o = \pi/2$. When defining a piston speed $V_p = V_o$ for the closing of the leakhole valve, it is to be expected that it will close the first time for $\omega t = \alpha_o$.
For increasing rpm the piston will run faster and the SCL will close at smaller angles (α_1, α_2 ... etc.). Corresponding with this closing the pump torque Q_p will vary as follows. (See fig. 4.3.)

$$Q_{ideal} = \rho_w \, g \, H \, A_p . \; \tfrac{1}{2} \, s \sin \omega t \quad \text{for } \alpha < \omega t < \pi$$
$$Q_{ideal} = 0 \quad \text{for } \pi < \omega t < 2\pi$$

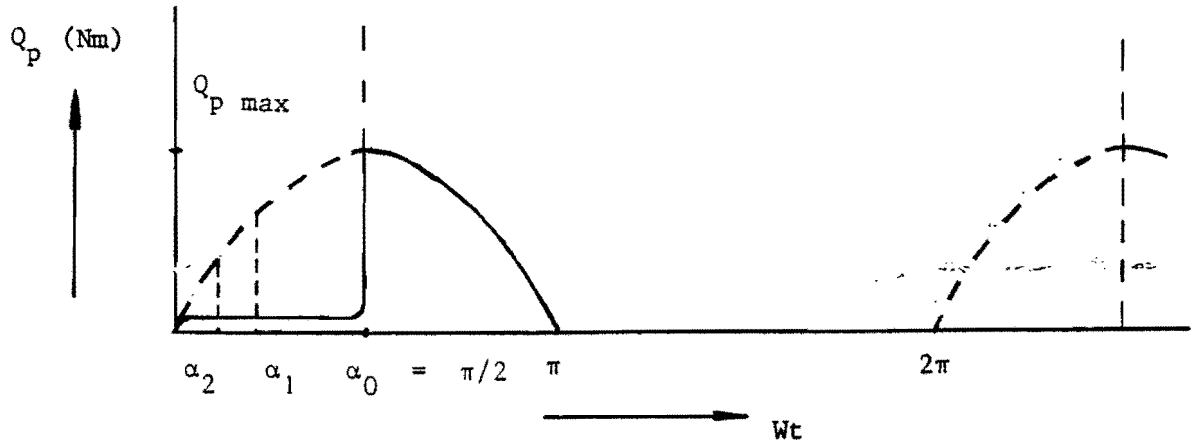

Fig. 4.3. The pump torque corresponding with the SCL closing

Integrating this instantaneous torque over a full circle gives the expression for the average torque.

$$\overline{Q}_p = \frac{\cos \alpha + 1}{2\pi} \rho_w g H A_p \tfrac{1}{2} s$$

This means that the first time the SCL will close (when $V_p = V_o$) the average pump torque will be:

$$\overline{Q}_p \ \alpha = \alpha_o = \frac{1}{4\pi} \rho_w g H A_p s \qquad (4.1.)$$

Which is exactly half the ideal average pump torque $\overline{Q}_{p\ ideal}$. (See fig. 3.1.) So the SCL has to be adjusted in such a way that the leakhole closes at a rpm ($n = n_s$) at which the rotor is able to exceed only half the $\overline{Q}_{p\ ideal}$. (See fig. 4.4.)

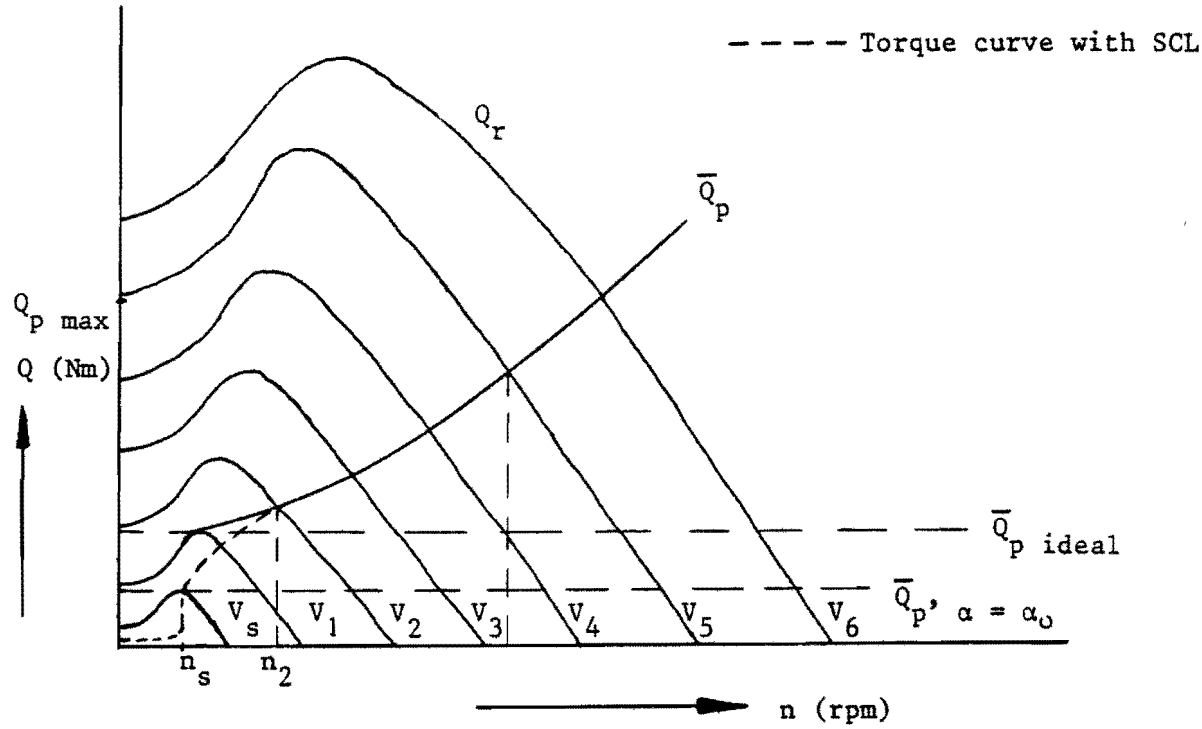

Fig. 4.4. Torque-rpm curves for rotor and pump with SCL-system

For increasing rpm as a result of increasing wind speed the pump torque will increase corresponding with the SCL closure angle. Theoretically the closure angle of the SCL (α_{SCL}) comes nearer to the closure angle of the piston valve (α_{cl}) for increasing rpm. So it is to be expected that for higher rpm the $\overline{Q}_p$ (as well as the η_{vol}) of the pump with a SCL will approximate the $\overline{Q}_p$ (and η_{vol}) of a pump with no starting provision. (See fig. 4.4)

5.1. The design of SCL I

Since at THE a pump test-rig with a CWD 145 pump was available it was decided to test a SCL on this pump.
Already a lot of measurements, without any starting provision as well as with a leakhole of ϕ 3 mm in the piston, were done on this pump. Most were done with a stroke of 0,08 m and a static lifting head of $\pm$ 10 m.

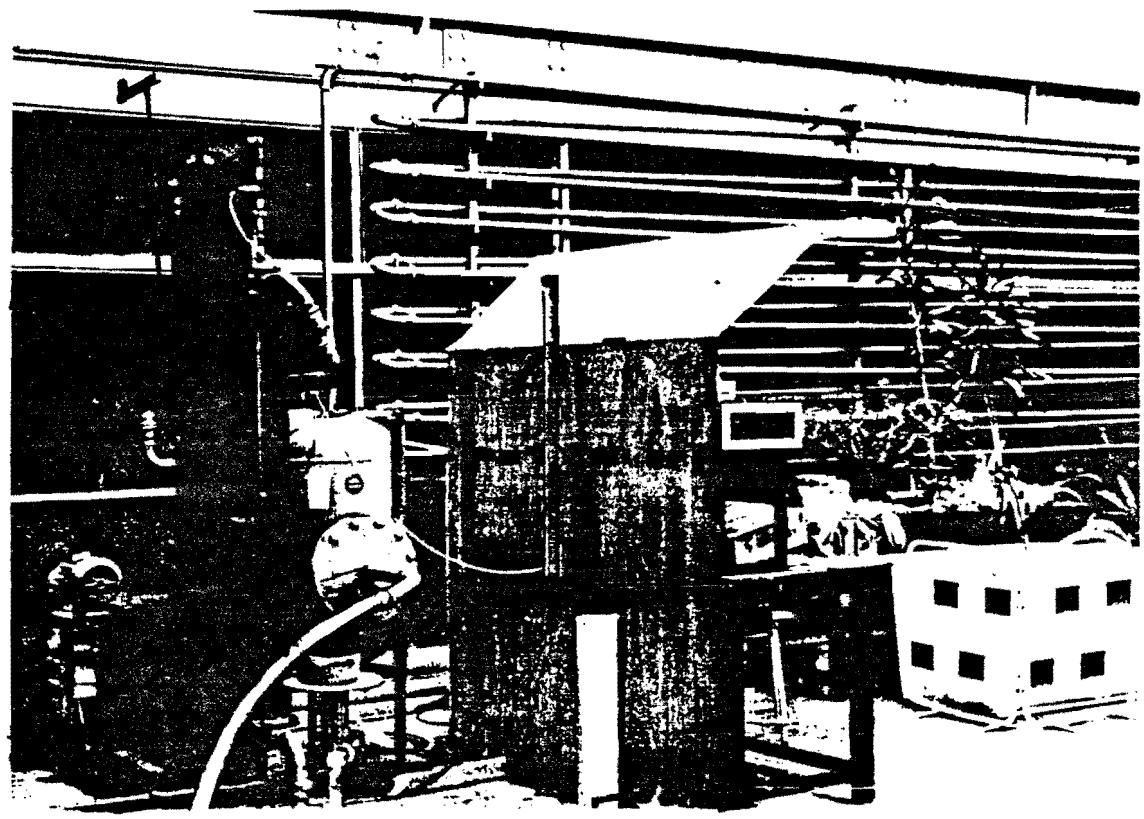

Pump test-rig at THE

In order to have good reference measurements it was decided to test the first SCL under these circumstances too. This means that the torque which the rotor has to exceed, when the SCL closes, must be:

$$\overline{Q}_{p,\ \alpha = \alpha_0} = \frac{1}{4\pi} \rho_w\ g\ H\ A_p\ s \quad \text{(see expression 4.1.)}$$

with:

$\rho_w = 10^3$ kg/m^3

$g = 9{,}8$ m/s^2

$H = 10$ m

$Ap^* = \frac{\pi}{4} dp = 1{,}54 \cdot 10^{-2}$ m^2

$s = 0{,}08$ m

$$\overline{Q}_{p,\ \alpha = \alpha_0} = 9{,}6 \text{ Nm}$$

In the torque-rpm characteristic of the rotor for increasing wind speed the corresponding rpm has to be gathered. For instance in fig. 4.4. the rotor torque exceeds the $\overline{Q}_{p,\ \alpha = \alpha_0}$ for $V_w = V_s$ and at a rpm of $n = n_s$.
The calculated $\overline{Q}_{p,\ \alpha = \alpha_0} = 9{,}6$ Nm however is not so realistic

for the CWD 2740 windmill, since this starting torque implies an ideal average torque of 19,2 Nm, which is rather high for this windmill. Besides the maximum stroke of the CWD 2740 is 0,06 m. So it is assumed that a windmill is available which is able to exceed a torque of 9,6 Nm at $\omega = 1$ rad/s ($n \approx 0{,}16$ rps). Consequently the SCL has to close at a $V_{p,\ max} = V_o$ corresponding with $\omega = 1$ rad/s. We know that $V_p = \frac{1}{2} s\omega \sin \omega t$. So for:

$$\omega = 1 \text{ rad/s}$$
$$s = 0{,}08 \text{ m}$$
$$\omega t = \pi/1$$

the closing speed will be $V_o = 0{,}04$ m/s. Supposing that all the water displaced by the piston flows through the SCL-system as long as it does not yet close, implies that the SCL has to close at a flow of:

$$\Phi_{close} = V_o . A_p \approx 0{,}62 \ . \ 10^{-3} \text{ m}^3/\text{s}$$

* The CWD 145 pump on the test-rig appeared to have a piston diameter of 0,14 m instead of 0,145 m.

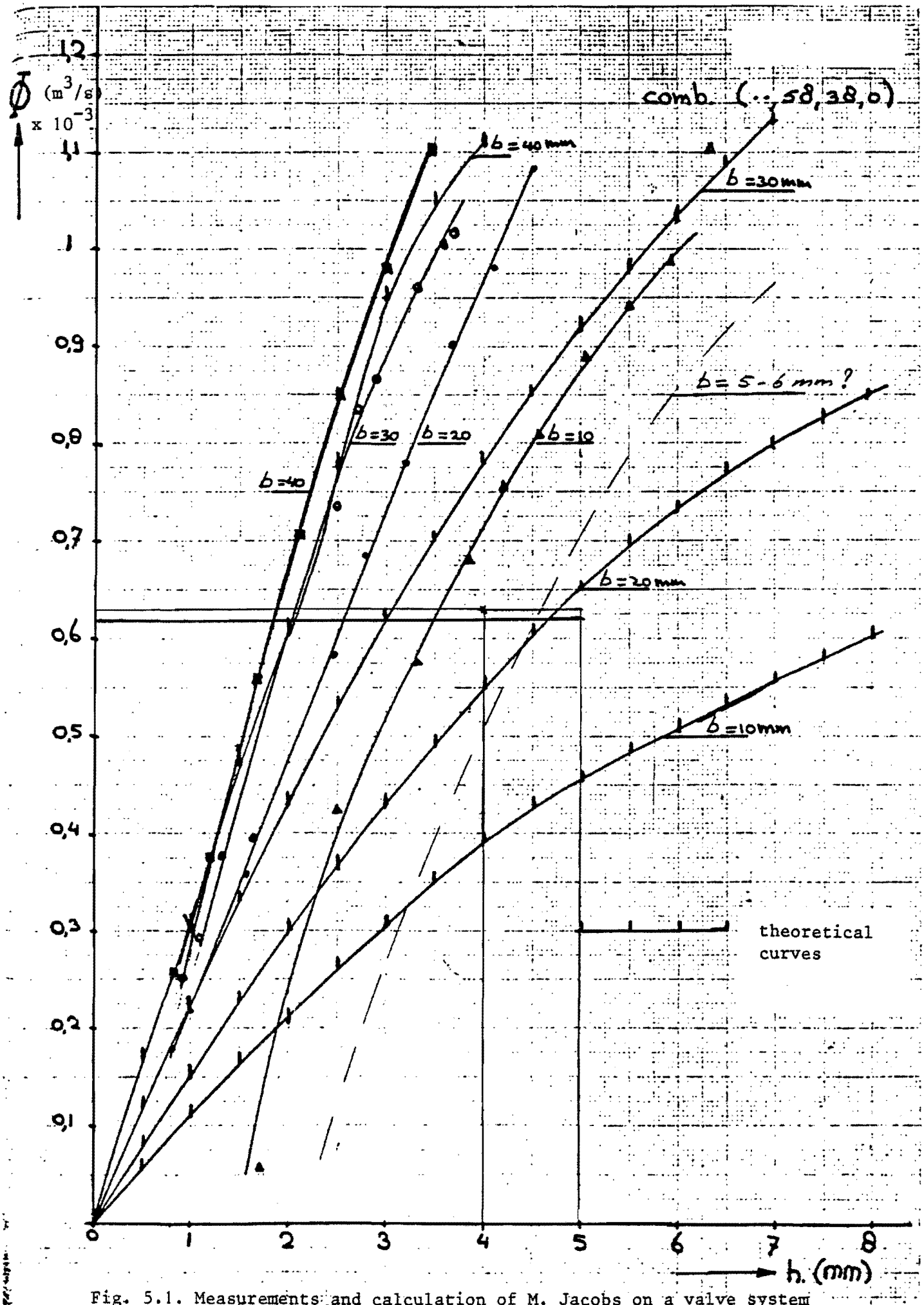

Fig. 5.1. Measurements and calculation of M. Jacobs on a valve system with several valve thickness b.

As argued in chapter 4.1. it is reasonable to use the measurements of M. Jacobs to define the first dimensions of the SCL. In fig. 5.1. the measured and calculated closure of a certain valve system is given, for several thickness b of the valve and for increasing valve gap height h. Increasing h and b demands a higher flow to close a certain valve system. For the sake of an acceptable height construction a valve of at most 5 or 6 mm thickness would be preferable.
As a consequence when the valve has to close at a flow of about $0{,}62.10^{-3}$ m^3/s a valve gap height of 4 to 5 mm is needed.
Using the dimension indications found above and taking into account the same surrounding areas as in the construction of M. Jacobs, a first SCL system is designed as shown in fig. 5.2.

The final essential dimensions of this SCL I are:

thickness valve	b = 5 mm
valve mass	m = $8{,}8.10^{-2}$ kg
gap height	h = 5 mm

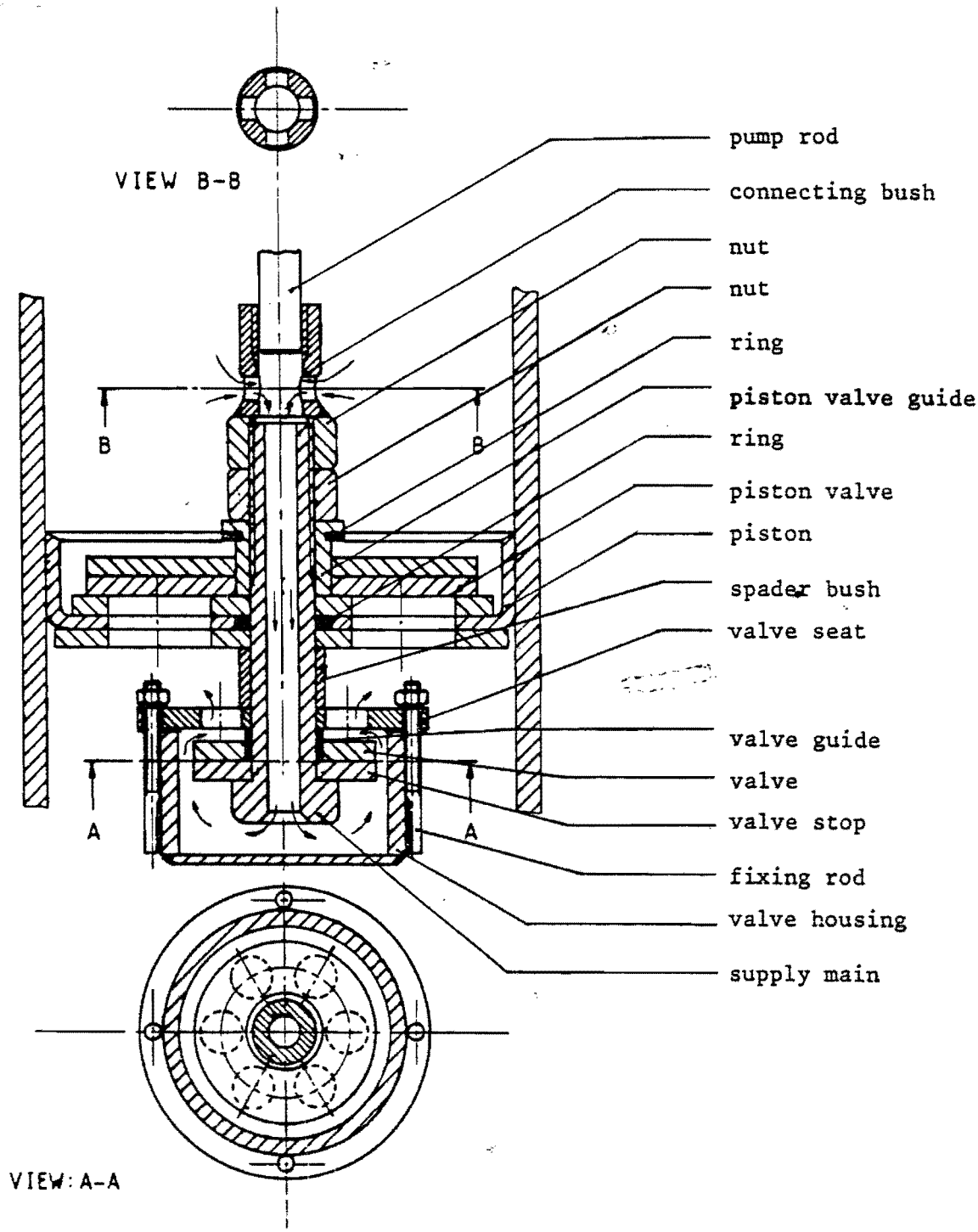

Fig. 5.2. The SCL-system

5.2. The test results of SCL I

This construction is tested in the CWD 145 pump at the pump test-rig at THE.
In the framework of this report it leads too far to give detailed information of this test-rig. It is sufficient to refer to the report of H. Meulenbroeks and E. Staring (Lit. 3) and the report of B. v. Noordwijk (Lit. 4). Besides an outline of the complete test-rig is drawn in fig. 5.3.

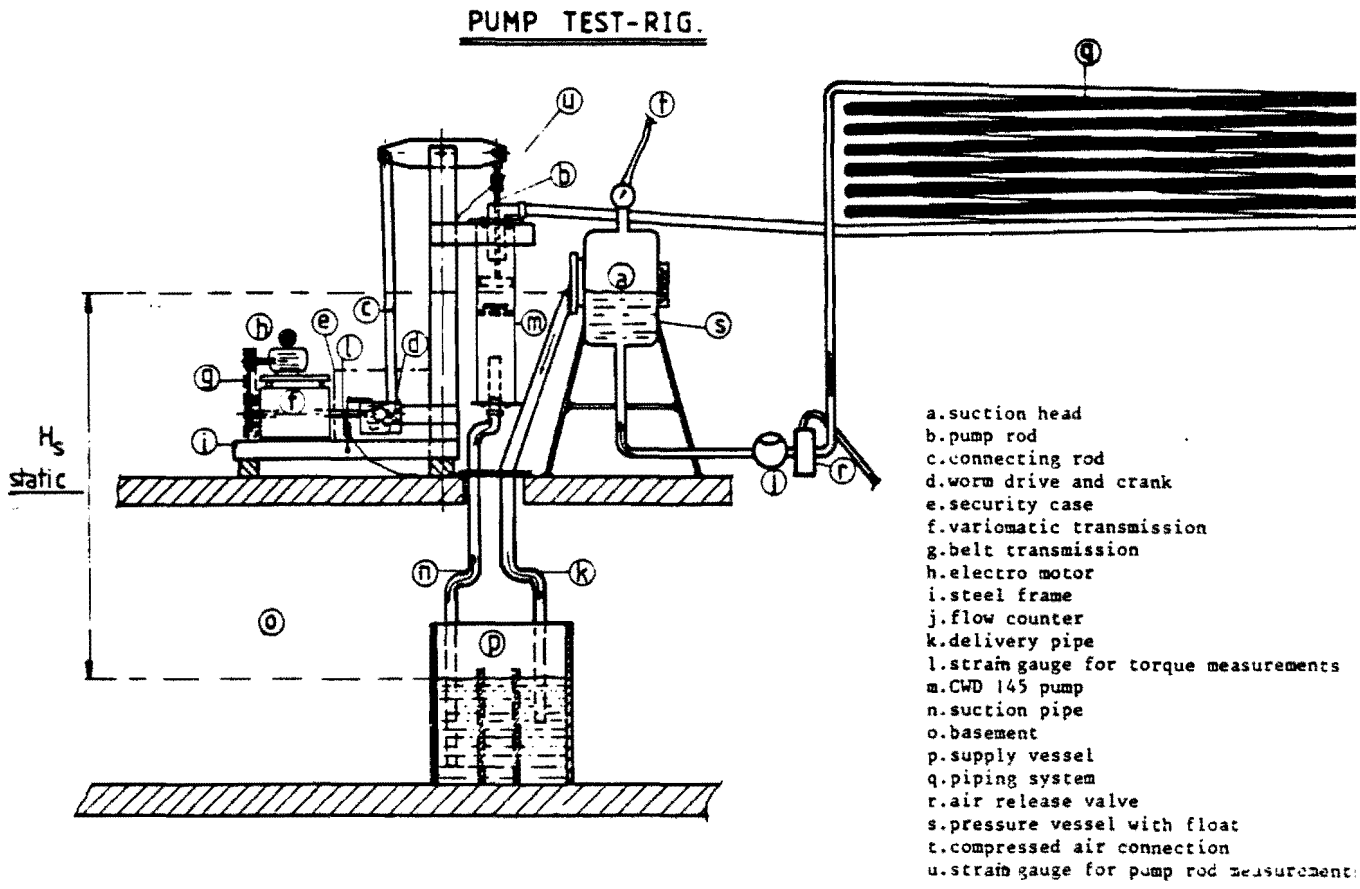

Fig. 5.3. The pump test-rig

Important is only that this test-rig has the facility to measure the following magnitudes:

- the pump-rod force as a function of ω
- the pump torque as a function of ω
- the average pump torque
- the output of the pump
- the rotational speed
- the BDC of the piston.

Specially for this SCL measurements two facilities were added:
- the valve closure angle of the piston could be measured directly by a "Hall-Effect" digital switch (see appendix 1)
- the valve closure angle of the SCL could be measured directly by a proportional "Hall-Effect" IC. (See appendix 2)

The results of these measurements are given in the tables A1 and A2 in appendix 3, and graphs A1, A2 and A3 appendix 4. For the sake of good comparison in all graphs measurements on the same pump with no leakhole and with a leakhole of ϕ 3 mm* are shown too.
The clonclusions of the first measurements can be:
- SCL I starts closing at n = 0,24 rps, (see graph A1) which is at a higher rps than expected. Notice however that, before the SCL closes, the pump starts to deliver, meaning that not all the water displaced by the piston flows through the SCL-system
- fig. 5.4. shows the valve closure angles of the SCL as a function of the rps. It is obvious that the closing does not come up to the expectation that for increasing rps the SCL would close sooner. This probably explains the low values of $\overline{Q}$, Q_{max} and the volumetric efficiency η_{vol} (see graphs A1, A2 and A3).

* This leakhole was drilled in the piston, but appeared to be too small. Later another leakhole of ϕ 3 mm is added.

For the leaving condition of the valve we can say that
$\zeta = \dot{\zeta} = \ddot{\zeta} = 0$

so:

$$Fst = m_v \ddot{x} + m'_v \; g \qquad (5.1.)$$

We know that:

$$\left.\begin{aligned} x &= A - A \cos \omega t) \\ \dot{x} &= A\omega \sin \omega t \;\;) \\ \ddot{x} &= A\omega^2 \cos \omega t \;\;) \end{aligned}\right. \qquad (5.2.)$$

$(A = \frac{1}{2} s)$

Assuming that all water displaced by the piston streams through the SCL untill it closes. We can suppose that the steady drag force is something like:

$$Fst = C \; Vp^2 = C \; \dot{x}^2 \qquad (5.3.)$$

C = unknown coefficient
Vp = velocity piston $(m.s^{-1})$

Substitution of equation (5.2.) and (5.3.) into (5.1.) gives:

$$CA^2 \omega^2 \sin^2 \omega t = m A \omega^2 \cos \omega t + m'g$$

Substitution of $\sin^2 \omega t = 1 - \cos^2 \omega t$ gives:

$$\cos^2 \omega t + \frac{m}{CA} \cos \omega t + \left(\frac{m'g}{CA^2 \omega^2} - 1\right) = 0$$

$$\text{So } \cos \omega t = \frac{-\frac{m}{CA} \pm \sqrt{\frac{m^2}{C^2A^2} - 4\left(\frac{m'g}{CA^2 \omega^2} - 1\right)}}{2} \qquad (5.4.)$$

To find a solution we know that:

$$\frac{m^2}{C^2A^2} - \frac{4\, m'g}{CA^2 \omega^2} + 4 \geq 0$$

This leeds to:

$$\omega \geq \sqrt{\frac{4\ m'g}{\frac{m^2}{C} + 4\ CA^2}}$$

To find C the measurements give us the border condition for n = 0,24 rps when the valve closes the first time.

$$2\pi.0,24 = \sqrt{\frac{4.7,7.10^{-2}.9,8}{\frac{8,8^2.10^{-4}}{C} + 4C.16.10^{-4}}}$$

$$\begin{aligned} n &= 0,24 \text{ rps} \\ m &= 8,8.10^{-2} \text{ kg} \\ m^1 &= 7,7\ 10^{-2} \text{ kg} \\ A &= \tfrac{1}{2}S = 0,04 \text{ m} \end{aligned}$$

So:

$$C \simeq 200$$

Back to equation (5.4.) we can say that for $\omega > 1,51$ rad/s this valve will lose at α_1, when

$$\cos \alpha_1 = \frac{-\frac{m}{CA} \pm \sqrt{\frac{m^2}{C^2A^2} - \frac{4\ m'g}{CA^2\ \omega^2} + 4}}{2}$$

Substituting the values of the valve gives:

$$\cos \alpha_1 = -\ 0.55.10^{-2} \pm \sqrt{1 - \frac{2.4}{10^2}}$$

The only usefull solution is the one with the plus sign.

Registration of the displacement of the SCL-valve (see appendix 2) proved that a neglectable mistake is made by assuming that the leaving angle is equal to the closure angle of the SCL-valve.
Since fig. 5.4. shows now this theoretical α_{scl} as a function of n, we can conclude that the acceleration force does not delay the closure of the SCL for increasing rpm. So the most acceptable reason for the disfunctioning of SCL I is a high resistance in the supply to the valve-system. Hence it is recommendable to decrease this resistance.

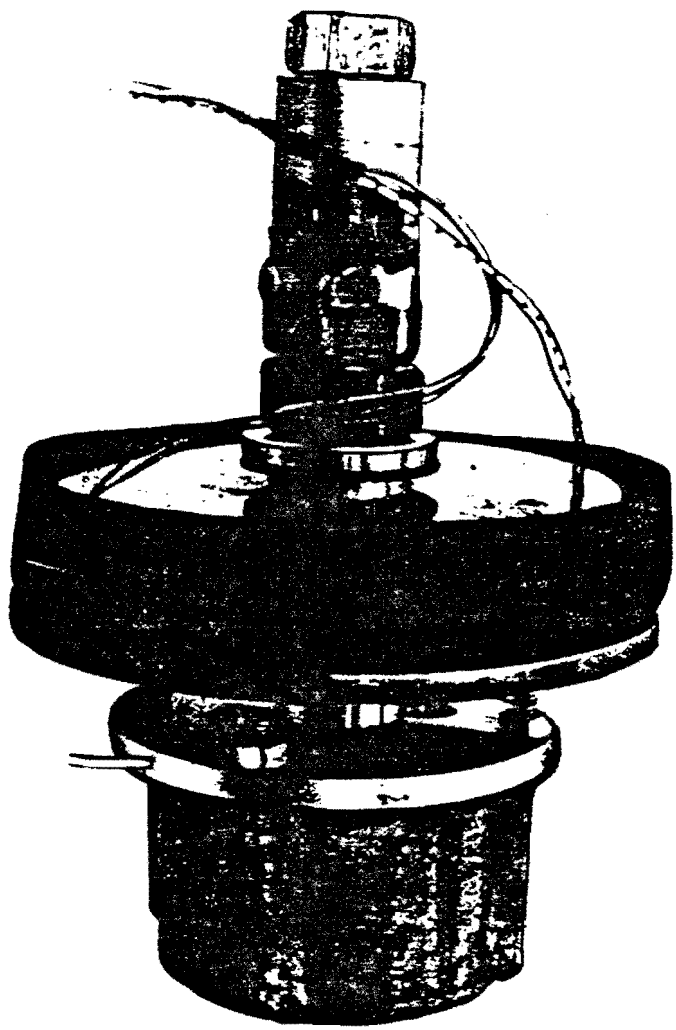

The SCL-system under the piston

6.1. The dimensions of SCL II

Summarizing the test results of SCL I we can conclude that first of all the supply to the valve-system has to be improved. That is why the diameter of the supply main (fig. 5.2.) has been increased from ϕ 10 mm to ϕ 12 mm.
In order to check the validity of the acceleration force calculation in chapter 5.2. it was decided to test a lighter valve than the one used in the SCL I-system.
But because of that lighter valve it was supposed that this SCL probably too early would start closing. Hence it was decided to use a thicker valve. All together the essential dimensions of SCL II are now:

thickness valve	b = 6 mm
mass valve	m = $1{,}8.10^{-2}$ kg
gap height	h = 5 mm
diam. supply main	D = 12 mm

6.2. The test results of SCL II

The results of the measurements are given in table A3 appendix 3. In order to compare them with the other measurements these results are also shown in graphs A1, A2 and A3, appendix 4.

From the test results the following conclusions can be drawn:

- SCL II starts closing at n = 0,073 rps, (see graph A1) which is earlier than the expected 0,16 rps (assumed in chapter 5.1.)
  Supposing that the decreasing of the valve mass dominates the increasing of the valve thickness could explain this problem
- fig. 6.1. shows the valve closure angle of SCL II as a function of n.

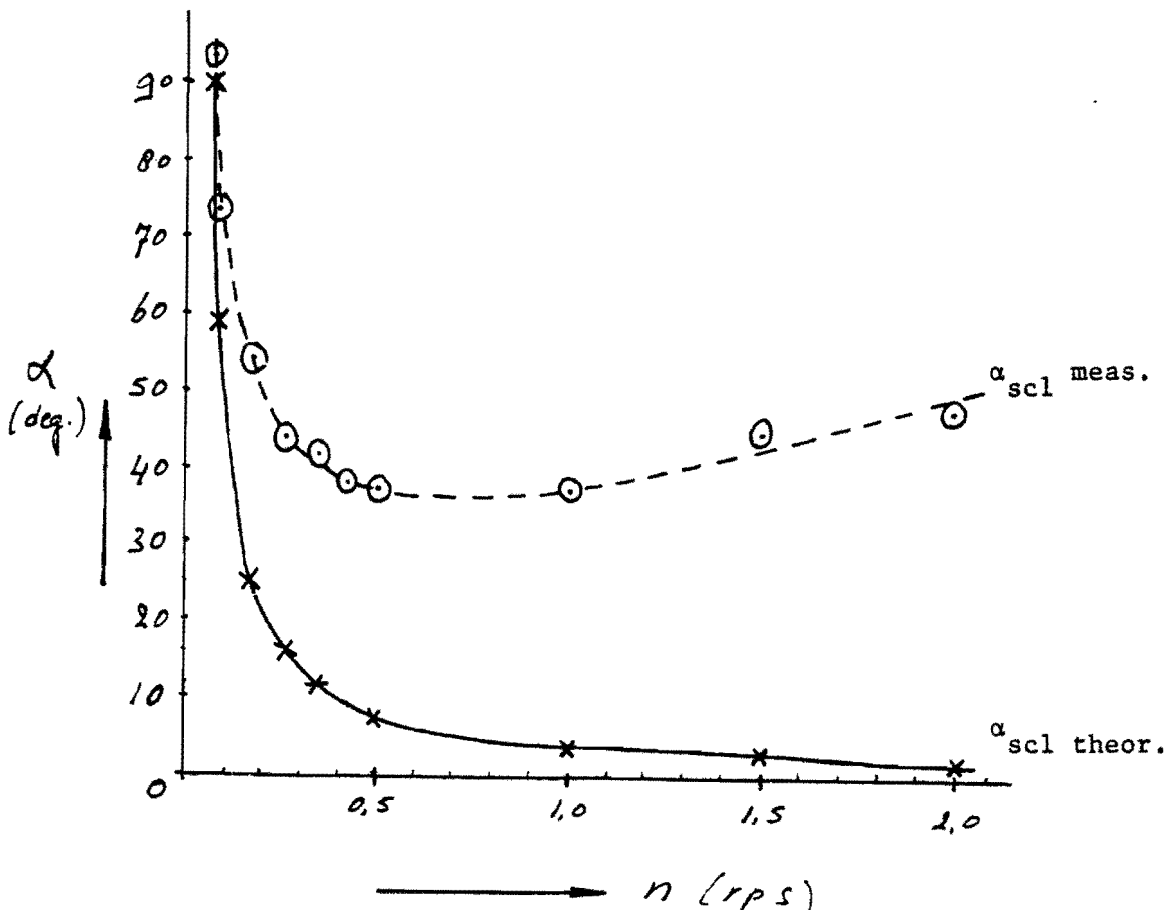

Fig. 6.1. The theoretical and measured valve closure angle of SCL I as a function of n

According to the measurements the closure angle α_{scl} decreases firstly, but then increases again for increasing rps. For a good comparison the theoretical closure angle is drawn too in this graph. Between these two curves there is still a great discrepancy. Hence it looks as if using this lighter valve is not really an improvement. It looks more as an indication that still somehow the resistance of the supply to the valve is too high.

In order to find out where this high resistance is situated in the SCL and to be able to solve this problem, it was decided to do stationary measurements on the complete SCL-system.

7. Sationary measurements

In order to perform the stationary measurements on the SCL, a special construction was made, according to the sketch of fig. 7.1.

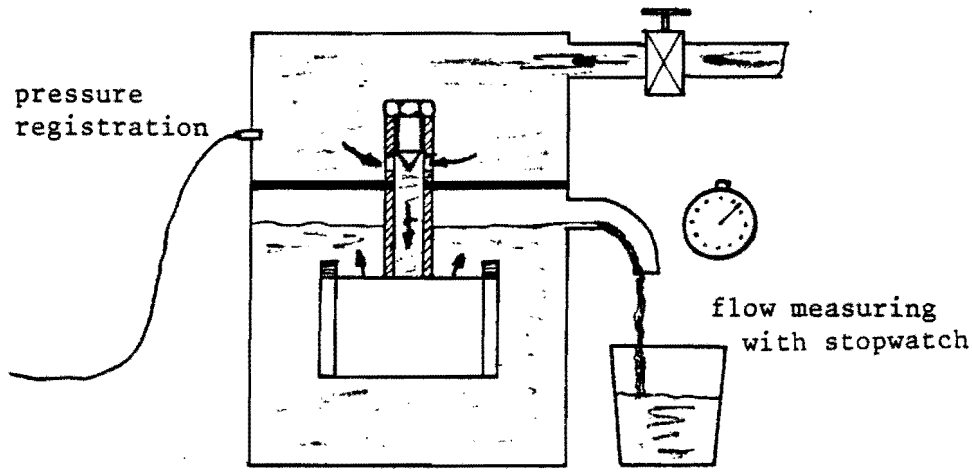

Fig. 7.1. Measuring the SCL resistance

With this construction it was possible to measure the pressure difference over the SCL-system and the flow through the system. Since the configuration of SCL II was not really an improvement, it was decided to measure on the SCL I construction.
In order to notice which modification really was an improvement, the SCL supply was changed and measured step by step. The measured results are given in tables B1, B2 and B3 appendix 3 and worked out in the graphs B1 and B2 of fig. 7.2. and fig. 7.5.

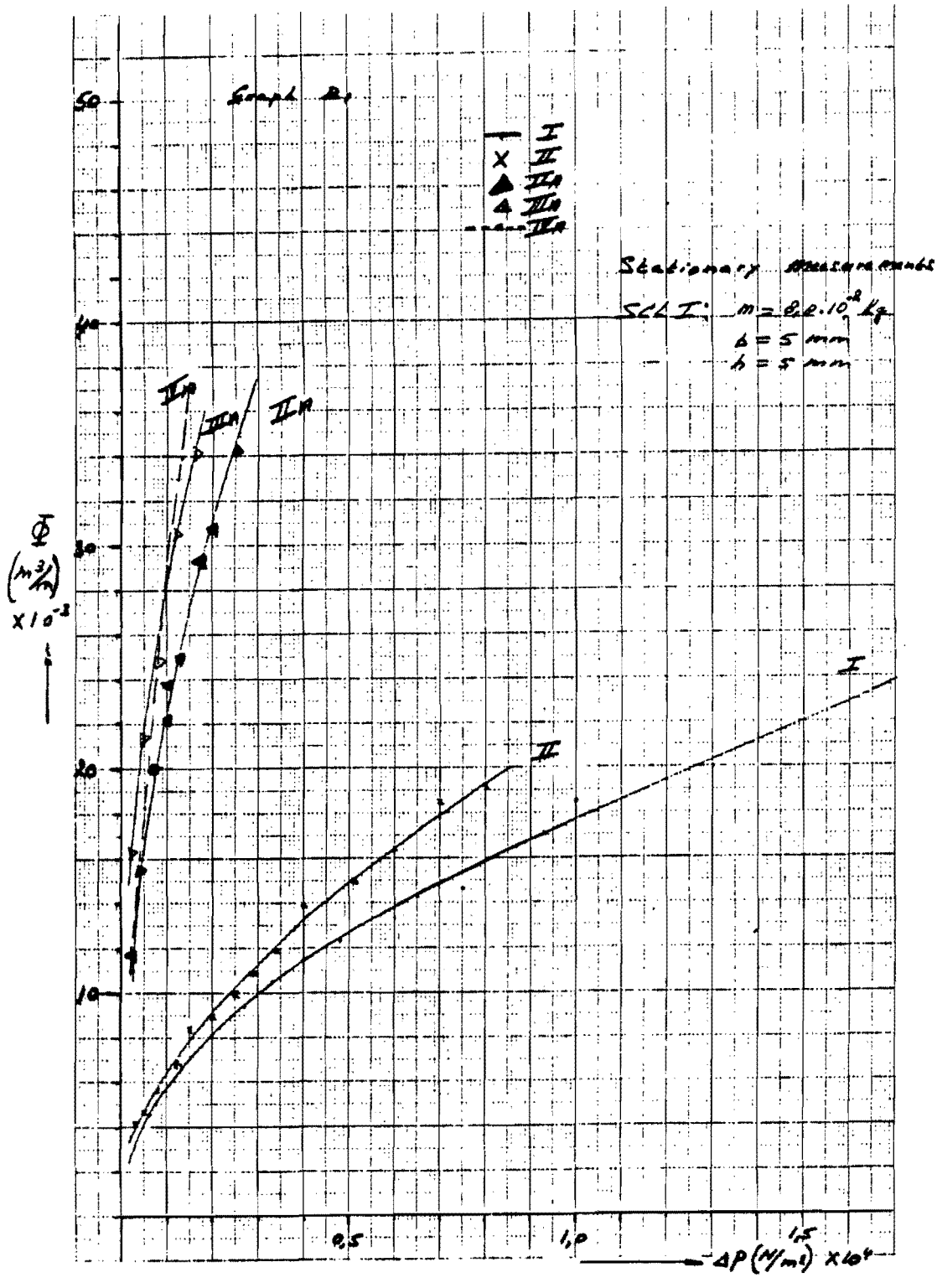

Fig. 7.2. Stationary measurements on SCL I

The best way to analyse the results is to follow the executed modifications step by step:

- curve I in fig. 7.2. gives the measurement on the original SCL I
- increasing the diameter of the supply main from 10 mm to 12 mm yields curve II
- changing the supply stream in the connecting bush by a tapered bolt (see fig. 7.3.) gives the improvement from curve II to curve II_A.

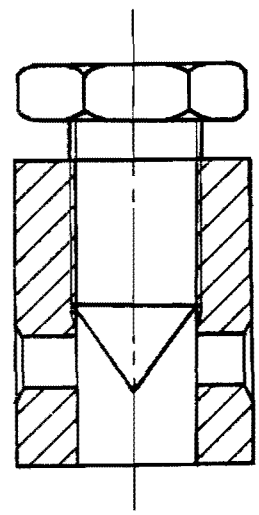

Fig. 7.3. Connecting bush with tapered bolt

- again increasing the diameter of the supply main (keeping the tapered bolt) yields curve III_A
- special adaptations are made to improve the supply of the SCL. See fig. 7.4.

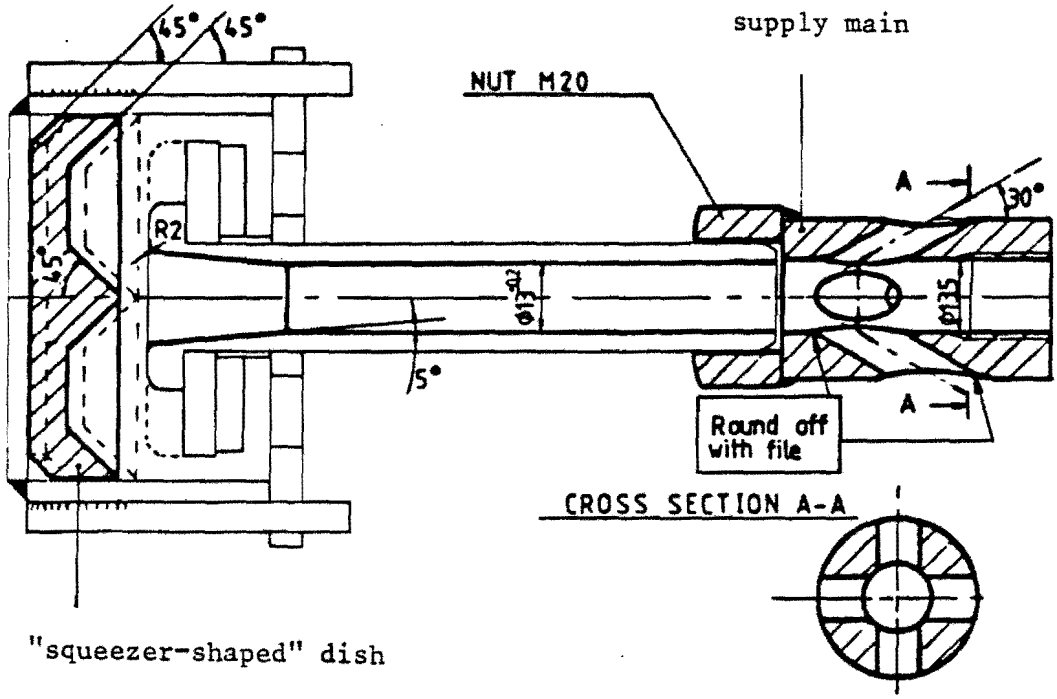

"squeezer-shaped" dish

Fig. 7.4. Adaptations for SCL

Measurements on the special connecting bush with inclined supply holes gives curve IV_A.

- The measurements in fig. 7.5. show the influence of the "squeezer-shaped" dish in the valve housing on the supply resistance.

Notice the other scale of Δp.

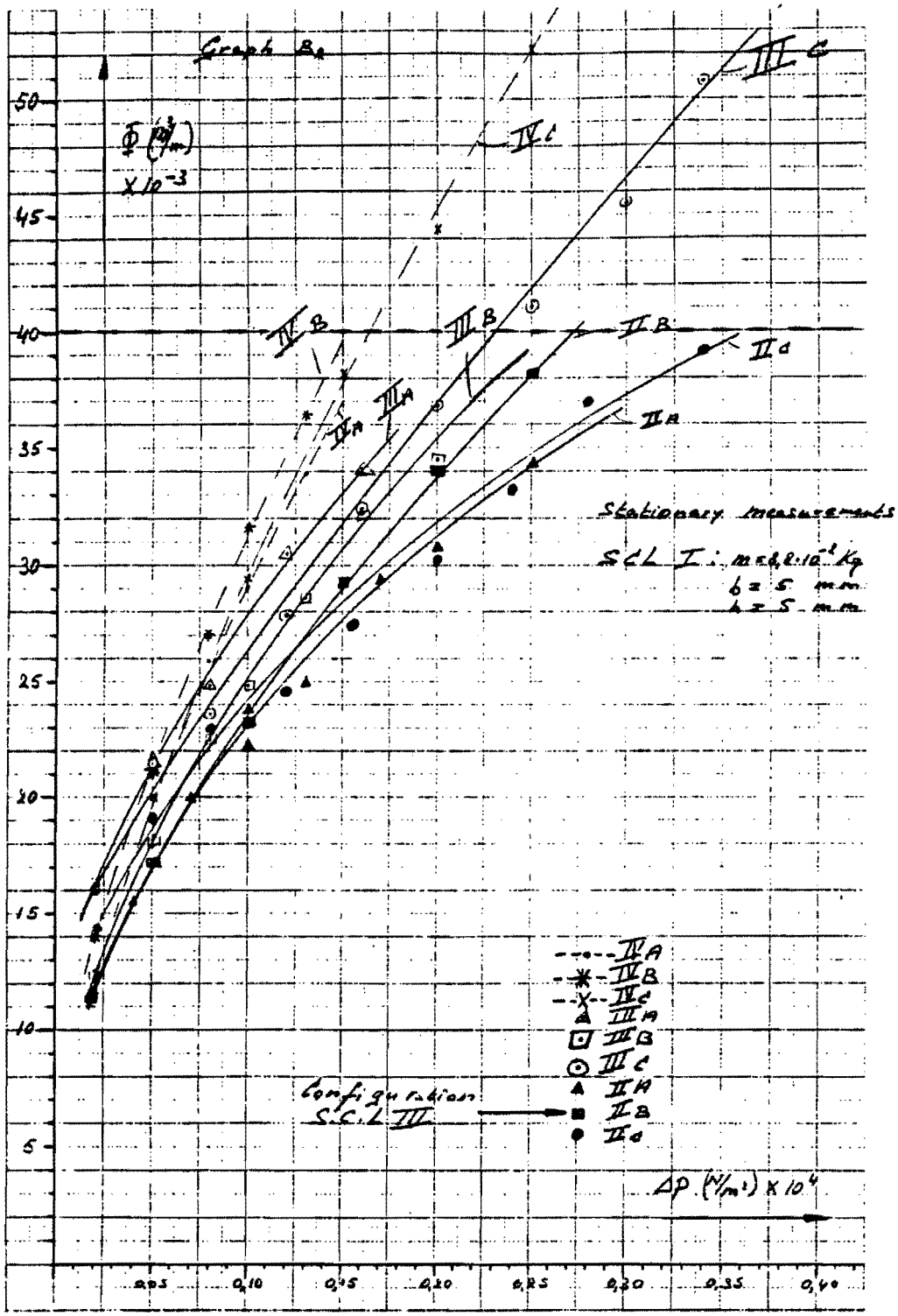

Fig. 7.5. Stationary measurements on SCL I

The meaning of the indices are:

A: no dish used

B: a dish of 2 mm thickness used

C: a dish of 10 mm thickness used

D: a dish of 12 mm thickness used

Summarizing the measurements warrant the following conclusions:

- reducing the resistance of the supply stream in the connecting bush is the most effective improvement.
  Compare II with II_A.
  For higher flows the improvement achieved by the inclined holes is a bit better than by a tapered bolt. Compare III_A with IV_A, and II_A with II_B.
- increasing the diameter of the supply feeder gives also an improvement. Compare I with II and II_A with III_A. But the strength of the construction (pump rod force) limits this increasement
- using dishes does not cause high improvements. Sometimes even the opposite.
  Compare III_A with III_B and III_C.

On account of this results a SCL III is selected (combination II_B) to test in the CWD 145 pump again.

8.1. The dimensions of SCL III

It is interesting to notice that according to the stationary measurements all systems, except III_C and IV_C, closed at a flow ϕ_{close} between $0{,}6.10^{-3}$ m^3/s and $0{,}66.10^{-3}$ m^3/s. According to the calculation in chpater 5.1. the SCL had to close at a flow of $\phi_{close} \approx 0{,}62.10^{-3}$ m^3/s. So it looks as if the reasoning leading to this calculation is right, meaning that it is in principle correct to use the measurements of M. Jacobs as an indication for the SCL dimensions. Hence, using the combination II_B (fig. 7.5.) it is reasonable to forecast that this SCL III will start closing at $n \approx 0{,}16$ rps as assumed in chapter 5.1.

Before testing SCL III however another remark has to be made: With regard to the delay of the closure of the SCL for increasing ω another phenomenon could be important. Lifting the SCL-valve from the valve stop takes some time, dependent on:

- the force Fst used
- the distance between valve and stop
- the contact surface between valve and valve stop

In lit. 5 an expression is found to calculate this phenomenon: (See appendix 5)

$$Fst = \frac{3\pi\ \eta\ \hat{h}\ R^4}{2h^3} \qquad \text{(see fig. 8.1.)}$$

η = dynamic viscosity (kg m^{-1} s^{-1})

$\eta_{water} = 10^{-3}$ kg/ms

This leeds to:

$$\int_{ho}^{h} \frac{dh}{h^3} = \int F^1 dt$$

$$F^1 = \frac{2\ F_{st}}{3\pi\ \eta\ R^4}$$

$$\frac{1}{2h^2} - \frac{1}{2h_o^2} = F^1 t$$

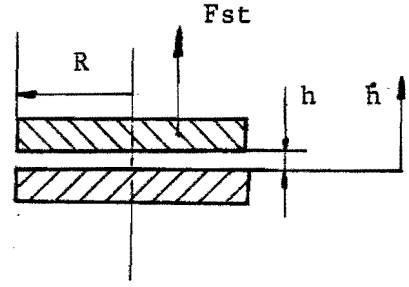

Fig. 8.1.

The boundary condition is ho = o, so:

$$t = \frac{1}{2\ F^1\ h^2} \qquad (6.1.)$$

Supposing that the contact surface is (see fig. 8.2.):

$$Av = \pi\ R^2 = \pi\ (r2^2 - r1^2)$$

We can, using the dimensions of the SCL-valve, assume that:

$$R \approx 2{,}6.10^{-2}\ m$$

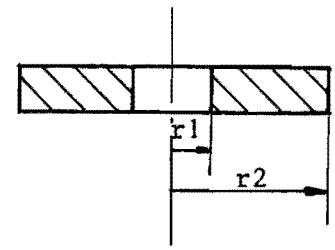

Fig. 8.2.

Back to equation (6.1.) and substitution of the known factors we find an expression for the time needed to lift the valve a certain distance with a certain force:

$$t \approx \frac{10^{-3}}{Fst.\ h^2}$$

Suppose that $Fst \approx 2.10^2\ \omega^2\ A^2\ Sin^2\ \omega t$ according to the calculation in chapter 3.4. To lift the valve for instance h = 0,1 mm this leeds to:

$$t = \frac{10^{-9}}{2.10^{-2}.\omega^2.4^2.10^{-4}\ Sin^2\ \omega t.10^{-8}}$$

So:

$$Sin\ \omega t = \sqrt{\frac{0{,}3125}{\omega^2 t}}$$

This can be solved by iteration.
To get an impression following table is made:

ω	t	α = ωt
1	0,72	0,72 rad = 41°
2	0,28	0,56 " = 32°
3	0,16	0,48 " = 28°
6	0,064	0,38 " = 22°
9	0,036	0,32 " = 19°
12	0,025	0,30 " = 17°

The last column gives the angle turning during the time the valve has been lifted the first 0,1 mm according to this estimation. It looks as if indeed this "stick-phenomenon" influences the valve-leaving. To avoid this phenomenon a ring has been turned off the bottom of the valve. See fig. 8.3.

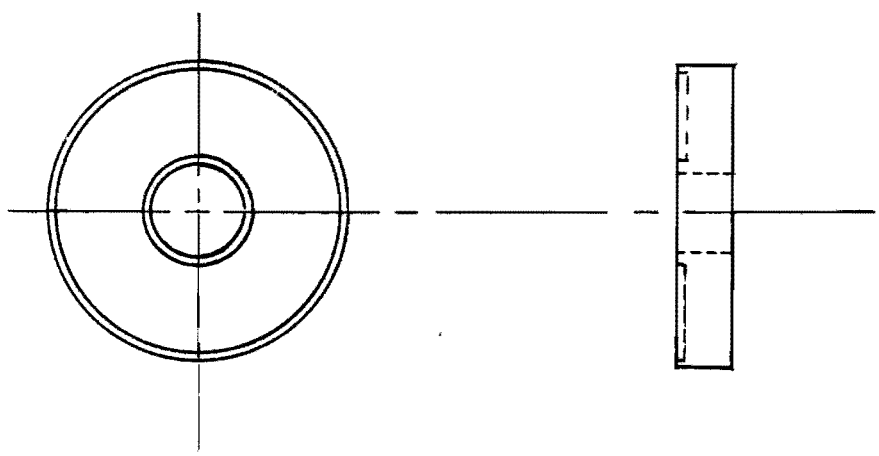

Fig. 8.3.

The original SCL III now will be called SCL III_A and the one like fig. 8.3. SCL III_B.
The essential dimensions of both are:

	SCL III a	SCL III b
thickness	b = 5 mm	b = 5 mm
gap height	h = 5 mm	h = 5 mm
mass	$m_v = 8{,}8.10^{-2}$ kg	$m_v = 8.10^{-2}$ kg
diam. supply feeder	D = 12 mm	D = 12 mm

Both have a connecting bush with sloping holes

8.2. The test results of SCL III

The results of SCL III a and III b are given in appendix 3 table C 1 and C 2.
In order to have a good comparison measurements under the same conditions with no leakhole and with two leakholes of ϕ 3 mm are made too. See table C 3 and C 4.
In the graphs C 1 - C 5 appendix 4 the results are worked out.

Before analysing these results, two remarks have to be made:
- the theoretic values of F_{max}, Q_{max} and $\overline{Q}$ are calculated with static head H = 10 m added with the dynamic head measured, for the test-rig, by M. Hilbers. (Lit. 7) See also appendix 6
- the theoretic α_{scl} values are calculated according to the same procedure as in chapter 3.4.

The results justify following conclusions:
- both SCL's start closing at a rotational speed of n = 0,17 rps, which is almost the calculated speed (see graph C 1)
- although both SCL's react more in a way we expected, they did not close sooner for increasing rotational speeds in spite of all adaptations. It also does not look as if the "stick-phenomenon" causes the delay (see graph C 3)
- both SCL-systems have about the same η_{vol} although SCL III a in general closes little earlier. On the other hand since SCL III a closes earlier $\overline{Q}$ is higher. The consequence is a lower $\eta_{ener.}$ for the SCL III a system (see graph C 1 and C 2)
- the F_{max} and Q_{max} of SCL III a are higher than those of SCL III b. We do not have an explanation for that (see graph C 4 and C 5)

Further analysis will be given in the discussion in chapter 8.

9. A check on the validity of the SCL design

In order to check the validity of these SCL test-series, we have tried to design a SCL according to the correct reasoning of chapter 4.2. and 5.1. based on the combination CWD 2740 windmill - CWD 145 pump.

A more realistic head of H = 5 m and the maximum stroke of s = 0,06 m are choosen.

The average torque demanded when the SCL starts closing is:

$$\tfrac{1}{2}\,\overline{Q} = \frac{1}{4\pi}\,\rho w\; g\; H\; A_p\; s$$

$$= \frac{1}{4\pi}.10^3.9{,}8.5.\frac{\pi}{4}.0{,}14^2.0{,}06$$

$$= 3{,}6 \text{ Nm}$$

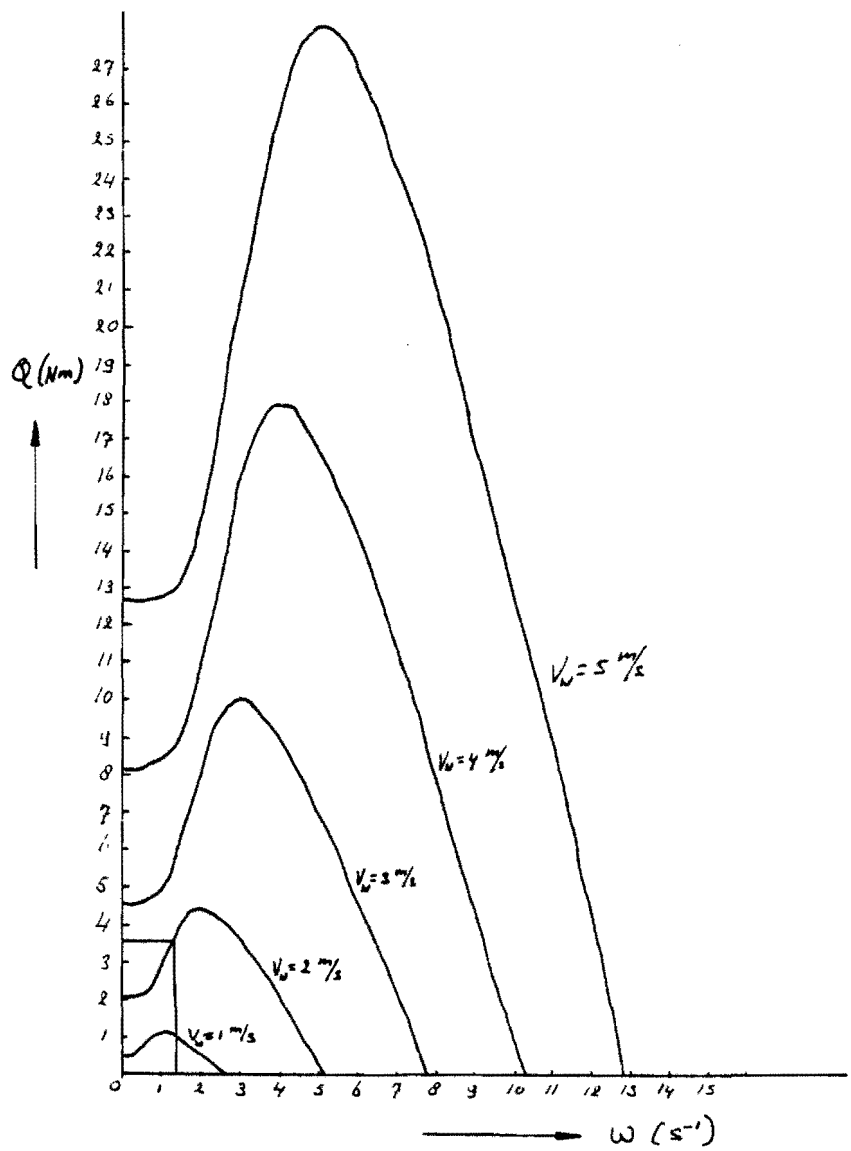

Fig. 9.1. The torque-ω characteristic of the CWD 2740 windmill

According to fig. 9.1. the CWD 2740 windmill is able to produce this torque at an angular velocity:

$$\omega \simeq 1{,}4 \text{ rad/s}$$

So:

$$V_o = \omega . \tfrac{1}{2} s = 0{,}042 \text{ m/s}$$

and:

$$\Phi_{close} = V_o . A_p . \simeq 0{,}65.10^{-3} \text{ m}^3/\text{s}$$

This happens to be the same as measured on the SCL in chapter 7. Which means that we can use the SCL III construction for this test-series.

Note:
Strictly the SCL construction had to be defined by means of the graphs of Jacobs. See fig. 5.1.

The test results of the reference measurements and SCL III b (the one used) are given in appendix 3 table D 1 - D 3.
In appendix 4 graph D 1 - D 5 the results are worked out.
Although the SCL-closure angles are little bigger, (obvious for smaller strokes) in general the results give the same picture as in chapter 8.2.

A few things are conspicuous:
- the low η_{vol} of the SCL-system compared with the normal leakhole. This is probably the consequence of the big closure angles α_{scl}. The $\eta_{ener.}$ of both is about the same
- the sharp fall of $\eta_{ener.}$ in all situations from a rotational speed of $n \simeq 0{,}7$ rps. This however is conform other measurements done at THE indicating that $\eta_{ener.}$ is clearly lower for smaller strokes
- the SCL indeed starts at $n \simeq 0{,}23$ rps, but the average torque is much higher as calculated. So in reality the SCL has to start at a higher n

10. Discussion

In the design of a SCL some progression is made since in principal we are able to design a construction of a leakhole that closes at a defined rotational speed.
Some prudence however is in place:

- first of all we must realise that the calculation of the average torque for Φ_{close} is based on the theoretical torque demanded by the pump. In reality the torque is higher as a result of frictions.
  Notice the high $\overline{Q}$ just before the SCL closes in graph C 1 and D 1 appendix 4
- the α_{scl} firstly decreases as expected, but from a certain rotational speed α_{scl} increases again. This is neither the consequence of acceleration forces nor of some "stick-phenomenon". Something else however is also interesting.
  In graph C 3 and D 3 the closure angle α_{cl} of the piston valve is worked out too.
  Notice now that α_{scl} theoretical is almost equal to α_{cl} when the α_{scl} starts increasing. This means that for higher n the piston valve is not yet closed when the SCL theoretically should close. And of course as long as the piston valve is not yet closed the SCL certainly will not close. But even then, the SCL-valve closes about 30^{o} later than the piston valve. So still there is somewhere in the system a delay causing that the SCL does not close immediately after the piston valve.
  Because for lack of time more research to solve this problem had to be left for someone else. Perhaps it is necessary to do some accurate pressure measurements in the cilinder to find an indication for this delay
- on the other hand it might be a better solution to develop an other SCL-system without this disadvantage.
  In connection with that one can think on several possibilities:
  - for instance a system with a provision preventing the SCL-valve to open again for higher rotational speed

- another possibility is to use the piston valve as a SCL-system. For instance by using springs, or by turning the complete pump construction. See fig. 10.1. on 10.2

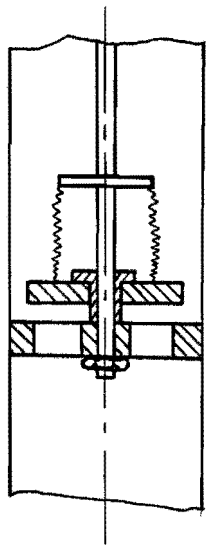

Fig. 10.1.

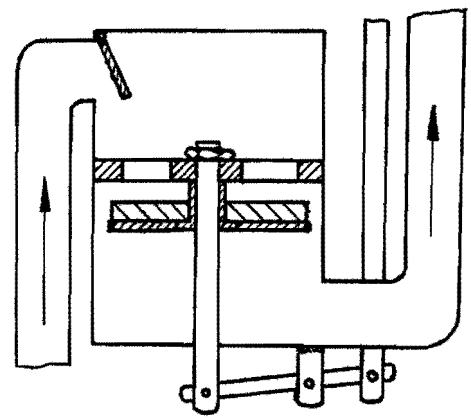

Fig. 10.2.

The piston valve used as a SCL-valve

11. Conclusions

Following the reasoning described in this report we are able to design a SCL which closes at the demanded rotational speed.

Unfortunately however the SCL-valve closes always about 30^{o} later than the piston valve.

It is necessary to do some more research to solve this problem in order to obtain higher volumetric efficiencies.

In case this problem can not be solved, it might be interesting to try another SCL construction as mentioned in chapter 10.

If it turns out not to be possible to improve volumetric efficiency the only advantage the SCL has with regard to a normal leakhole is a much lower starting torque.

It is important to remember that for smaller strokes the energetic efficiency is lower.

12. Literature

1. E.H. Lysen
Introduction to Wind Energy
CWD publication
August 1982

2. M. Jacobs
The speed controlled leakhole (in Dutch)
Internal report, R-594-A
June 1983

3. H. Meulenbroeks & E. Staring
Measurements and calculations on a single acting piston pump to be used for windmills (in Dutch)
Internal report, R-527-S
April 1982

4. B. v. Noordwijk
Pump rod forces of the "Tanzania pump" measured and calculated (in Dutch)
Internal report, R-609-S
1983

5. L.D. Landau & E.M. Lifshitz
Fluid Mechanics
Institute of physical problems
U.S.S.R. Academy of science
Pergamon Press
1959

6. M. Hilbers
Three different measurements on a test-rig for the "Tanzania" pump (in Dutch)
Internal report, R-644-S
December 1983

SPRAGUE
THE MARK OF RELIABILITY

INTEGRATED CIRCUIT
ENGINEERING BULLETIN

UGN-3013T

TYPE UGN-3013T SOLID-STATE ULTRA LOW-COST 'HALL EFFECT' DIGITAL SWITCHES

FEATURES:

- Operate from 4.5 V to 16 V d-c power source.
- Activates with small, commercially available permanent magnets.
- Solid-state reliability — no moving parts.
- Small size.
- Constant amplitude output.
- Output compatible with all digital logic families.

THE SPRAGUE TYPE UGN-3013T is a low-cost magnetically-activated electronic switch. Each device consists of a voltage regulator, a Hall voltage generator, amplifier, Schmitt trigger, and an open collector output stage integrated in a single monolithic silicon chip.

The on-board regulator permits operation over a wide variation of supply voltages. The circuit output can be interfaced directly with bipolar or MOS logic circuits.

UGN-3013T integrated circuits are packaged in the miniature 3-pin single output plastic "T" pack.

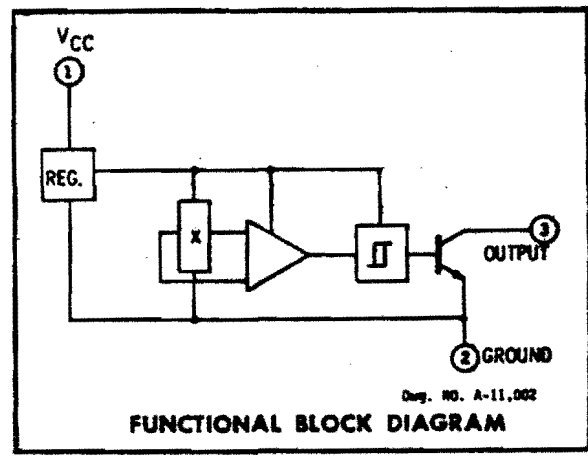

FUNCTIONAL BLOCK DIAGRAM

ABSOLUTE MAXIMUM RATINGS

Power Supply, V_{CC} ..... 17 V
Magnetic Flux Density, B ..... Unlimited
Output "OFF" Voltage, $V_{OUT(OFF)}$ ..... 17 V
Storage Temperature Range, T_S ..... −65°C to +150°C
Operating Temperature Range, T_A ..... 0°C to +70°C
Output "ON" Current, I_{SINK} ..... 40 mA

ELECTRICAL CHARACTERISTICS: V_{CC} = 4.5 V to 16 VDC, T_A = 25°C

Characteristic	Symbol	Test Conditions	Limits			Units
			Min.	Typ.	Max.	
Magnetic Flux Density "Operate Point", "Release Point"	B_{OP} B_{RP}		— 25	300 225	450 —	Gauss Gauss
Hysteresis	B_H		30	75	—	Gauss
Output Saturation Voltage	V_{SAT}	B ≥ 450 Gauss, I_{SINK} = 15 mA	—	120	400	mV
Output Leakage Current	I_{OFF}	B ≤ 25 Gauss, V_{OUT} = 16 V	—	.1	20	μA
Supply Current	I_{CC}	V_{CC} = 5 V, output open	—	7	9	mA
		V_{CC} = 12 V, output open	—	12	16	mA
Output Rise Time	t_r	V_{CC} = 12 V, R_L = 820 Ω, C_L = 20 pF	—	15	—	ns
Output Fall Time	t_f	V_{CC} = 12 V, R_L = 820 Ω, C_L = 20 pF	—	100	—	ns

TYPE UGN-3013T
'HALL EFFECT' DIGITAL SWITCHES

Catalog Numbering System

UG N - 3013 T

- T — PACKAGE STYLE. T = PLASTIC 3-LEAD SIP
- 3013 — DEVICE NUMBER. 3000 – 3199 = DIGITAL, SINGLE OUTPUT
- N — OPERATING TEMPERATURE RANGE. N = 0°C TO +70°C
- UG — SEMICONDUCTOR FAMILY. UG = HALL EFFECT DEVICES

DIMENSIONS IN INCHES

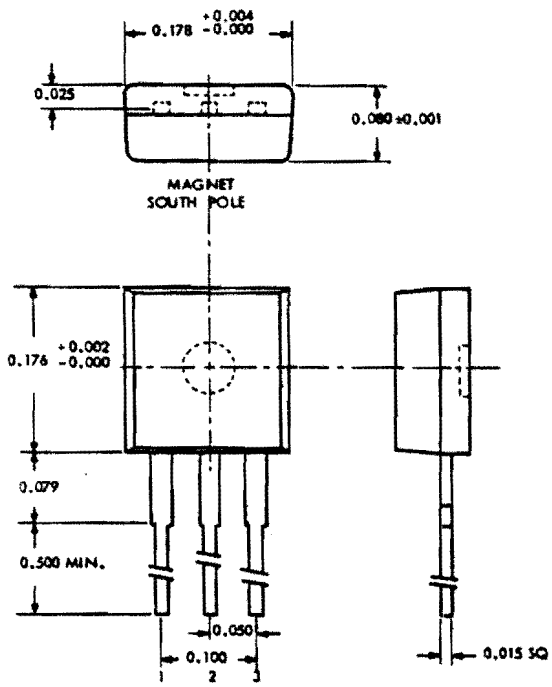

NOTES: 1. All dimensions are in inches.
2. Hall cell is centrally located.

Dwg. No. A-9761A IN

DIMENSIONS IN MILLIMETRES

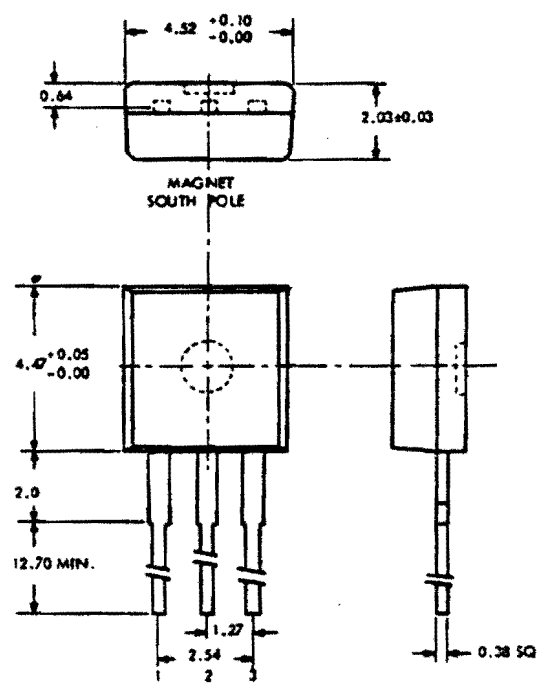

NOTES: 1. All dimensions are in millimetres
2. Hall cell is centrally located.

Dwg. No. A-9761A MM

GUIDE TO INSTALLATION

1. All Hall effect integrated circuits are susceptible to mechanical stress effects. Caution should be exercised to minimize the application of stress to the leads or the epoxy package.

2. To prevent permanent damage to the Hall cell I.C., heat sink the leads during hand soldering. For wave soldering, the part should not experience more than 230°C for more than 5 seconds and no closer than 0.125" to the epoxy package.

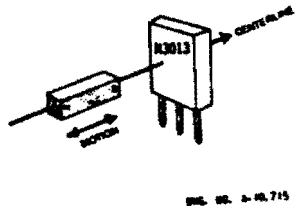

BASIC 'HEAD-ON' MODE OF OPERATION

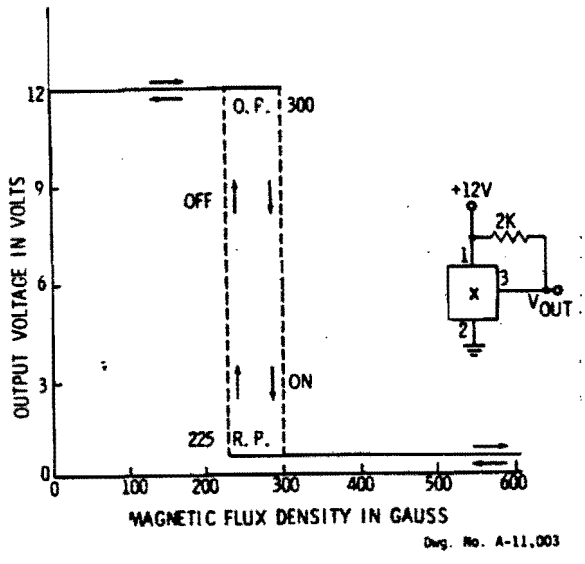

TRANSFER CHARACTERISTICS SHOWING HYSTERESIS

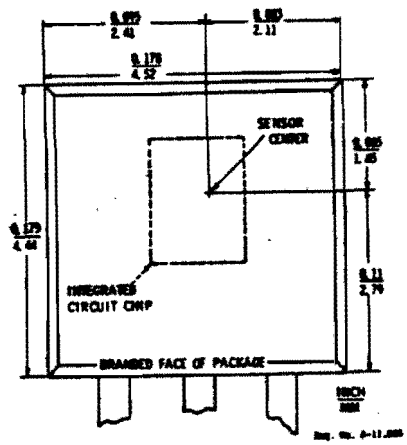

SENSOR CENTER LOCATION

OPERATION

The output transistor is normally "off" when the magnetic field perpendicular to the surface of the chip is below the threshold or "operate point." When the field exceeds the "operate point," the output transistor switches "on" and is capable of sinking 15 mA of current.

The output transistor switches "off" when the magnetic field is reduced below the "release point" which is less than the "operate point." This is illustrated graphically in the transfer characteristics curve. The hysteresis characteristic provides for unambiguous or non-oscillatory switching.

The simplest form of magnet which will operate the Hall effect digital sensor is a bar magnet as shown. Other methods are possible.

In the illustration, the magnet's axis is on the center line of the packaged device and the magnet is moved toward and away from the device. Also, note the orientation of the magnet's south pole in relation to the branded face of the package.

The magnetic flux density is indicated for the most sensitive area of the device. This area is centrally located and 0.032" ±0.002" (0.81 ±0.05 mm) below the branded surface of the package.

For reference purposes, both an Alnico VIII magnet, 0.212" (5.38 mm) in diameter and 0.187" (4.75 mm) long and a samarium cobalt magnet, 0.100" (2.54 mm) square and 0.040" (1.02 mm) thick, are approximately 1200 gauss at its surface.

The flux density decays at a high rate as the distance from a pole increases.

As an example, using the Alnico VIII magnet referenced above in good alignment and the pole surface in contact with the branded surface of the package, the flux density at the active Hall sensing area of the device would be approximately 850 gauss (0.032" below the package surface).

The flux density would drop to approximately 600 gauss with an air-gap between the package and the magnet of 0.031" (0.79 mm).

For additional information on Hall Effect device applications, see Sprague Engineering Bulletin No. 27701, "Hall Effect Applications Guide."

Die Bausteine SAS 241, SAS 250, SAS 251, SAS 261 sind magnetisch betätigte kontaktlose Schalter mit folgenden Betriebsarten:

Typ	Kennzeichnung	Speisespannungsbereich	Funktion
SAS 241	SAS 241	4,75 bis 18 V	Schalter, dynamisch
SAS 241 S4	weiß	4,75 bis 5,25 V	offene Kollektorausgänge
SAS 250	SAS 250	4,5 bis 27 V	
SAS 251	SAS 251	4,75 bis 27 V	Schalter, statisch
SAS 251 S4	SAS 251 S4	4,75 bis 5,25 V	offene Kollektorausgänge
SAS 251 S5	orange	4,75 bis 18 V	
SAS 261	blau	4,75 bis 18 V	Schalter; statisch
SAS 261 S4	grün	4,75 bis 5,25 V	offener Kollektorausgang und Freigabeeingang

Alle Bausteine sind im vierpoligen Flachgehäuse lieferbar. SAS 241 und SAS 251 sind auch als filmmontierte Ausführung im MIKROPACK auf Anfrage lieferbar.

Der Baustein SAS 231 liefert eine Spannung proportional zur magnetischen Induktion. Er ist aufgrund seiner MIKROPACK-Bauform besonders für einen Betrieb in sehr kleinen Luftspalten geeignet.

Typ	Kennzeichnung	Speisespannungsbereich	Funktion
SAS 231 L	–	4,75 bis 15 V	Hall-IS mit magnetfeldproportionaler Ausgangsspannung MIKROPACK
SAS 231 W	blau/grün	4,75 bis 15 V	Hall-IS mit magnetfeldproportionaler Ausgangsspannung Miniaturgehäuse

Typ	Bestellnummer	Gehäusebauform
SAS 231 L	Q 67000 - A 1468 - L	MIKROPACK
SAS 231 W	Q 67000 - A 1468-W	Miniaturgehäuse 6 Anschlüsse

Der Baustein SAS 231 liefert am Ausgang eine Spannung proportional zur magnetischen Induktion (Flußdichte). Die Ausgangsspannung nimmt zu, wenn der Südpol eines Magneten der Chipoberseite genähert wird. Der Nullpunkt wird durch externen Abgleich eingestellt. Die Steilheit der Kennlinie $U_Q = f(B)$ kann durch externe Beschaltung variiert werden.

Grenzdaten		Prüfbedingungen	untere Grenze B	typ	obere Grenz A	Einheit
Speisespannung	U_S		0		18	V
Ausgangsstrom	I_Q				10	mA
Lagertemperatur	T_s		-40		125	°C
Funktionsbereich						
Speisespannung	U_S		4,75		15	V
Ausgangsstrom	I_Q				5	mA
Umgebungstemperatur im Betrieb	T_U		0		70	°C
Statische Kenndaten bei U_S = 10 V, T_U = 25 °C, wenn nicht anders angegeben						
Leerlaufstromaufnahme	I_S	R_L = ∞		6	10	mA
Ausgangsspannung	U_Q	R_L = 10 kΩ	0,05		U_S - 2	V
Steilheit (ohne Abgleich)	S		60	100	140	mV/mT
„Null"-Komponente	B_0	U_Q = 0,5 V	-35		35	mT
Linearitätsfehler (bezogen auf $U_Q = \frac{U_S}{2}$)				2		%
Temperaturkoeffizient	α	T_U = 0 ... 70 °C		0,4		mT/K

Anschlußanordnungen

SAS 231 W

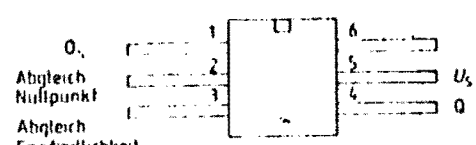

SAS 231 L

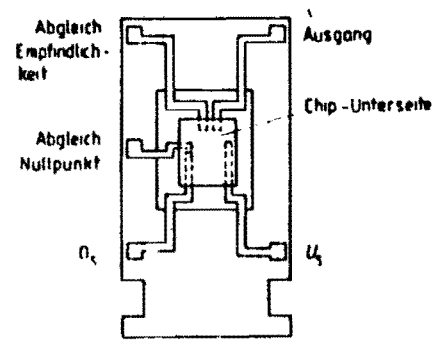

Anwendungsschaltung

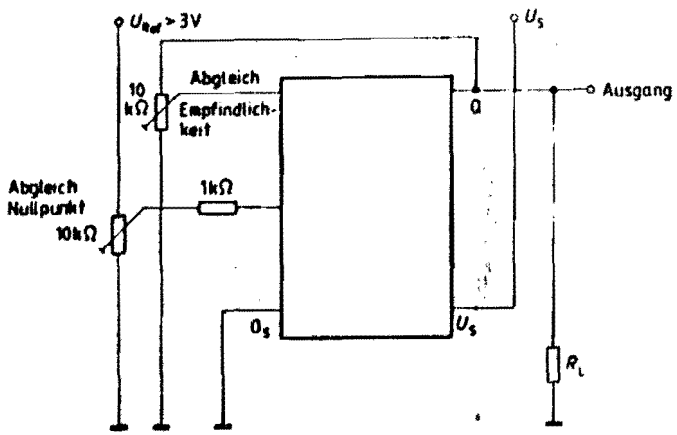

Ausgangskennlinie ohne Abgleich $U_Q = f(B)$

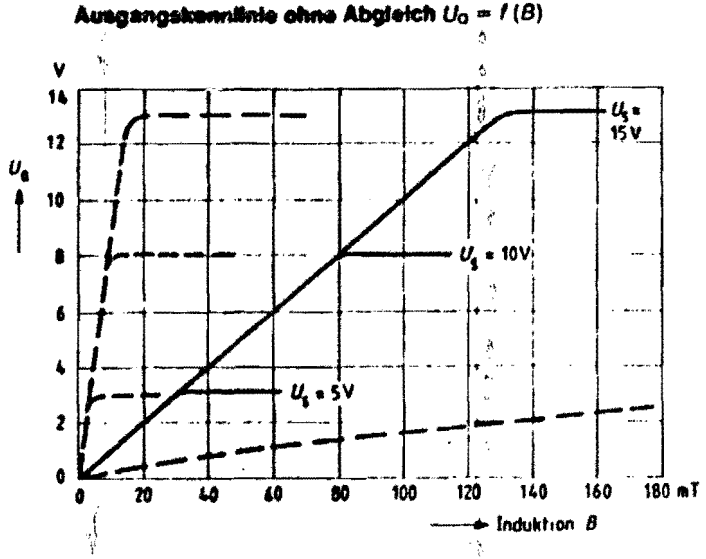

Table: A.1																	Stroke Vol: $1{,}23 \cdot 10^{-3}\ m^3$
Date: 30-11-'83	Measurements on CND 145 With SCL I																Stroke: 9,08 m
Head: ± 10 m Measur. nr: II	n (rpm)	n (rps)		Φ ($\times 10^{-2}$) (m^3/m)	Φ ($\times 10^{-3}$) (m^3/s)	η_{vol} (%)	F_{max} (N)			Q_{max} (Nm)	$\bar{Q}$ (Nm)		α_{CL} (deg)	α_{SCL} (deg)		Comments.
1	13	0,22		0	0	0	1250			50	15,9		8	–		SCL - open
2	15	0,25		3,5	906	13,5	1250			68	21,6		10	103		SCL - closed
3	20	0,33		9,2	0,15	36,6	2100			76	24,2		11	81		〃
4	30,5	0,51		17,1	0,29	46,4	2200			74	23,6		8	100		〃
5	39,9	0,67		26	0,43	52,6	2480			76	24,2		9	113		〃
6	49,8	0,83		35,8	0,6	58,8	2650			84	26,7		11	129		〃
7	59,9	1,0		44,4	0,74	69,3	2760			90	28,6		12	126		〃
8	79,1	1,17		53,5	0,89	61,9	3100			96	30,6		13	123		〃
9	80,1	1,34		62,5	1,04	63,3	3400			106	33,7		15	136		〃
10	90,1	1,5		70,5	1,18	63,9	3650			120	38,2		16	121		〃
										Calculated	Calculated					

Table: A: 2	(Low rps)															Stroke Vol: $1{,}83 \cdot 10^{-3}$ m³
Date: 2-12-'83	measurements on CWD 145 with SCL I															Stroke: 0,08 m
Head: ± 10 m	n	n					$F_{max.}$			Q_{max}	$\bar{Q}$		α_{cl}	α_{scl}		Comments.
Measur. nr: III	(rpm)	(rps)					(N)			(Nm)	(Nm)		(deg.)	(deg.)		
1	4	0,067					113			4,2	1,6		7	–		SCL – open
2	6,2	0,103					500			12,2	3,9		9	–		"
3	8,1	0,135					850			21,5	6,8		7	–		"
4	10,5	0,18					1070			28,6	9,1		11	–		"
5	12,2	0,20					1320			35,7	11,4		11	–		"
6	13,4	0,22					1530			41,2	13,3		10	–		"
7	14,2	0,24					1717	When SCL closes	1300 N	45,3	14,6		12	138		SCL sumtimes closed
8	14,9	0,25					1770			54,3	17,3		11	125		SCL. – closed
9	15,8	0,26					1950			62,9	20		14	94		"
											CWD outlet					

Table: A·3

Date: 10-1-'84

measurements on CWD 145 with SCL II

Stroke Vol: $123 \cdot 10^{-3}$ m³

Stroke: 0,08 m

Head: ± 10 m

Measur. nr: IV

	n (rpm)	n (rps)		$\bar{Q}$ ($\times 10^{-3}$) (m^3/m)	$\bar{Q}$ ($\times 10^{-3}$) (m^3/s)	η_{vol} (%)	F_{max} (N)			Q_{max} (Nm)	$\bar{Q}$ (Nm)		α_{cl} (deg.)	α_{scl} (deg.)		Comments.
1	5,1	0,085		0	0	0	1766			66,8	16,8		7	73		SCL - closed
2	10,1	0,17		3,3	0,055	26,3	2123			79,6	23,1		9	54		"
3	15,5	0,26		0,8	0,146	45,9	2335			83,2	27,1		5	44		"
4	20,6	0,34		13,2	0,22	52,5	2516			87,7	28,5		11	42		"
5	25,1	0,42		16,8	0,28	55	2882			98,9	30,4		12	38		"
6	29,8	0,50		22,8	0,38	61,4	3146			97,5	32,3		14	37		"
7	53,6	1.0		53,4	0,89	78,8	3831			116,3	39,4		10	37		"
8	92,0	1,5		82,2	1,37	72,8	5071			161,5	52,9		14	45		"
9	121,3	2,0		105	1,75	70,2	6506			203,8	65,4		13	48		"
Low rps 10	4,4	0,073		0	0	0	1513			5,3	3,4		5	33		SCL - CLOSED
11	3,8	0,063		0	0	-	242			5,7	3,8		5	-		SCL - open

table B.1	Steady drag force measurements on the S.C.L. I															$G = 0{,}88\,N$. $b = 5$ mm. $h = 5$ mm.
Date: 10-2-'84	I Original			II Original			II_A Special bolt no disk			$II_{B'}$ Special bolt disk 7 mm			II_B Special bolt disk 10 mm			
Opvoerh: —	Δp (N/m^2) $\times 10^4$	Φ (l/m)	—	Δp (N/m^2) $\times 10^4$	Φ (l/m)	×	Δp (N/m^2) $\times 10^4$	Φ (l/m)	▲	Δp (N/m^2) $\times 10^4$	Φ (l/m)		Δp (N/m^2) $\times 10^4$	Φ (l/m)	●	
Meting nr ✓																Comments
1	0,06	4,5		0,01	—		0,01	—		0,01	—		0,01	—		Series I:
2	0,13	6,8		0,03	4,1		0,02	11,7		0,05	11,8		0,02	14,0		Supply feeder ϕ 10
3	0,20	8,1		0,05	4,7		0,04	15,5		0,08	16,7		0,05	19,1		
4	0,27	9,4		0,08	5,6		0,07	20,0		0,12	21,3		0,08	23,0		Series II:
5	0,33	10,5		0,12	6,8		0,10	22,2		0,16	25,0		0,12	24,6		Supply feeder ϕ 12
6	0,40	11,5		0,15	8,4		0,10	23,8		0,20	27,4		0,16	27,5		
7	0,48	12,3		0,20	9,0		0,13	25,0		0,25	31,5		0,20	30,3		Series III:
8	0,60	13,3		0,25	10,0		0,17	29,4		0,30	35,1		0,24	33,3		Supply feeder ϕ 12
9	0,65	14,3		0,29	10,9		0,20	30,8		0,34	closed		0,28	37,0		
10	0,75	14,6		0,34	11,9		0,25	34,3					0,34	39,2		Series IV:
Series II_B 11	0,92	17,1		0,40	13,9		0,30	closed.		II_B	Special disk	Supply 2 mm ■	0,36	closed		Supply feeder ϕ 12
1 12	1,0	18,5		0,51	15,0					0,01	—					
2 13	1,3	20,0		0,60	16,4					0,02	11,5					
3 14	2,7	28,1		0,70	18,5					0,05	17,2					
4 15	4,0	32,4		0,80	19,2					0,10	23,3					
5										0,15	29,3					
6										0,20	34,1					
7										0,25	38,2					
8										0,28	closed		—	—	—	leak water 4,7 l/m.

table B.2 — Steady drag force measurements on the S.C.L. I

$Q = 0,88\ N$
$b = 5\ mm$
$h = 5\ mm$

date: 14-2-84

Opvoerh: —

Meting nr. —

	III A Spedial bolt no disk			III B Spedial bolt disk 2mm			III C Spedial bolt disk 10mm			III D Spedial bolt disk 12mm						
	Δp (N/m^2) $\times 10^4$	Φ (l/m)	△	Δp (N/m^2) $\times 10^4$	Φ (l/m)	⊡	Δp (N/m^2) $\times 10^4$	Φ (l/m)	⊙	Δp (N/m^2) $\times 10^4$	Φ (l/m)					Comments
1	0,01	—		0,01	—		0,01	—		0,01	—					Series III
2	0,02	16,3		0,02	12,3		0,02	16,2		0,03	13,8					Supply feeder ∅ 13
3	0,05	21,4		0,05	18,2		0,05	21,1		0,08	19,5					
4	0,08	24,8		0,08	22,5		0,08	23,6		0,15	28,8					
5	0,12	30,5		0,10	24,8		0,12	27,9		0,20	34,8					
6	0,16	34,1		0,13	28,6		0,16	32,4		0,25	40,3					
7	0,18	closed		0,16	32,3		0,20	36,8		0,30	42,9					
8				0,20	34,5		0,25	41,1		0,35	closed					
9				0,25	closed		0,30	45,5								
10							0,34	50,8								
11							0,39	closed								

Table B.3 — Steady drag forde measurements on the S.C.L. I

Date: 15-2-84

G. = 0,88 N
b = 5 mm
h = 5 mm

Opvoerh: — / Meting nr. —	IV A Special Supply No dish ΔP (N/m²) X10⁴	IV A Special Supply No dish Φ (l/m)	IV B Special Supply dish 2 mm ΔP (N/m²) X10⁴	IV B Special Supply dish 2 mm Φ (l/m)	IV C Special Supply dish 10 mm ΔP (N/m²) X10⁴	IV C Special Supply dish 10 mm Φ (l/m)	Comments
1	0,01	—	0,01	—	0,01	—	Series IV:
2	0,02	12,1	0,02	14,0	0,05	20,0	Supply feider Φ13
3	0,05	18,3	0,05	21,1	0,10	29,4	
4	0,08	25,9	0,08	27,1	0,15	38,2	
5	0,10	29,1	0,10	31,6	0,20	44,4	
6	0,13	33,9	0,13	36,4	0,25	52,2	
7	0,15	closed	0,15	closed	0,29	closed	

Table: C-1

Date: 26-3-'84

measurements on CWD 145 With SCL IIIa

Stroke Vol: $1{,}23 \cdot 10^{-3}\ m^3$

Stroke: 0,08 m

Head: ± 10m

Measur. nr: VI

	n (rpm)	n (rps)	$H_{tot.}$ (m)	Φ $\times 10^{-2}$ (m^3/m)	Φ $\times 10^{-3}$ (m^3/s)	η_{vol} (%)	F_{max} (N)		η_{ener} (%)	Q_{max} (Nm)	$\bar{Q}$ (Nm)		α_{CL} (deg.)	α_{SCL} (deg.)		Comments.
1	5	0,08	0	0	0	—	215		—	6,6	2,4		7	—		SCL. - open
2	10,1	0,17	0	0	0	—	530		—	13,0	6,2		10	—		SCL sometimes
2	"	"	10	4,5	0,08	36,2	2000		67	55,7	11,0		10	120		Closed
3	14,9	0,25	10,25	12,1	0,20	66,0	2310		54	78,0	23,7		9	66		SCL - Closed
4	20,0	0,33	10,5	18,8	0,31	76,4	2585		53	93,4	29,1		10	43		"
5	29,6	0,49	11,25	29,6	0,49	81,3	2990		52	104,6	34,0		11	40		"
6	39,3	0,66	12,15	40,0	0,67	82,7	3180		53	111,5	36,3		12	40		"
7	42,3	0,83	13,4	52,3	0,87	85,2	3550		56	121,5	38,8		12	37		"
8	59,4	0,99	14,75	62,5	1,04	85,5	3900		57	134,3	42,6		13	38		"
9	82,6	1,49	13,7	91,3	1,52	82,8	5090		55	182,9	57,2		16	43		"
10	111	1,85	25	113,2	1,89	82,9	6490		54	219,8	74,0		17	55		"

$$\eta_{vol} = \frac{\Phi}{n \cdot Ster.Vol.}$$

$$\eta_{mech.} = \frac{\rho_w g H \Phi}{\bar{Q} \cdot 2\pi n}$$

Table: C-2

Date: 28-3-'84 — measurements on CWD 145 with SCL III 6

Stroke Vol.: $1{,}23 \cdot 10^{-3}$ m³

Stroke: 0,08 m

Head: ± 10 m

Measur. nr.: VII

	n (rpm)	n (rps)	$H_{tot.}$ (m)	$\dot{Q}$ ($\times 10^{-3}$ m³/s)	$\bar{Q}$ ($\times 10^{-3}$ m³/s)	η_{vol} (%)	F_{max} (N)		η_{meter} (%)	Q_{max} (Nm)	$\bar{Q}$ (Nm)		α_{dl} (deg)	α_{scl} meas.	α_{scl} theor.	Comments.
1	5,3	0,08	–	0	0	0	248		–	8,0	3,7		4	–	–	SCL. – open
2	10,2	0,17	–	0	0	0	550		–	18,4	6,8		7	–	–	SCL sometimes
2	〃	〃	10	4,8	0,08	38,3	1940		46	64,7	16,0		7	96	90	closed
3	15,0	0,25	10,25	12,6	0,21	68,3	2215		60	74,3	22,4		6	69	43	SCL. – closed
4	20,0	0,33	10,5	18,6	0,31	75,6	2365		57	84,0	27,1		12	52	31	〃
5	30,1	0,50	11,4	31,2	0,52	84,3	2900		63	93,7	29,4		9	41	20	〃
6	40,0	0,67	12,3	42,0	0,70	85,4	3080		65	98,2	30,8		10	40	15	〃
7	50,1	0,84	13,5	52,8	0,88	85,7	3365		64	108,6	34,3		11	42	12	〃
8	59,8	1,0	14,75	61,8	1,03	84,0	3995		61	122,6	38,6		11	46	9	〃
9	82,4	1,49	20,0	92,4	1,54	84,0	4280		62	162,2	51,6		15	57	7	〃
10	112,8	1,88	25,6	115,2	1,33	83,0	6330		61	210,0	66,3		17	57	5	〃

Table: C.3	measurements on CWD 145 with no leakhole															Stroke Vol: $1{,}23 \cdot 10^{-3}$ m³
Date: 3-4-'84																Stroke: 0,08 m
Head: ± 10m	n	n	H_{tot}	$\bar{\Phi}$ $\times 10^{-3}$	$\bar{\Phi}$ $\times 10^{-3}$	η_{vol}	F_{max}		$\eta_{ener.}$	Q_{max}	$\bar{Q}$		α_{ol}			Comments.
Measur. nr: VIII	(rpm)	(rps)	(m)	(m^3/m)	(m^3/s)	(%)	(N)		(%)	(Nm)	(Nm)		(deg)			
1	6,1	0,10	10,1	7,8	0,13	100	2420		70	33,6	23,3		7			
2	9,8	0,16	10,25	12,6	0,21	100	2280		81	81,4	25,9		7			
3	15,1	0,25	10,5	18,6	0,31	100	2375		80	85,6	25,4		8			
4	23,9	0,33	10,8	24,0	0,40	98,1	2575		69	94,3	23,4		8			
5	29,5	0,49	11,75	35,4	0,59	97,6	3160		70	104,7	31,5		9			
6	40,6	0,67	13	48,6	0,81	97,3	3380		73	109,2	33,6		9			
7	50,0	0,83	14,5	60,0	1,00	97,6	3775		63	123,7	39,5		10			
8	60,1	1,0	16,2	71,4	1,19	96,6	4070		71	130,6	42,6		13			
9	90,2	1,5	22,6	103,2	1,72	93,0	5470		66	188,6	60,6		18			
10	105,6	1,76	27,0	120	2,00	92,4	6330		67	220,0	71,4		17			

Table: C-4	Measurements on CWD 145 with 2 leakholes ϕ 3 mm														Stroke Vol: $1{,}23 \cdot 10^{-3}$ m³
Date: 4-4-'84															Stroke: 0,08
Head: ± 10 m	n	n	$H_{tot.}$	Φ $\times 10^{-3}$	Φ $\times 10^{-3}$	η_{vol}	F_{max}		$\eta_{mech.}$	Q_{max}	$\bar{Q}$		α_{el}		
Measur. nr: ~~X~~	(rpm)	(rps)	(m)	(m^3/m)	(m^3/s)	(%)	(N)		(%)	(N m)	(N m)		(deg.)		Comments.
1	5,5	0,09	10	1,8	0,03	26,6	1325		24	74,0	22,0		7,5		
2	9,7	0,16	10,1	7,2	0,12	60,3	1905		53	71,4	22,3		7		
3	15,5	0,26	10,25	13,2	0,22	63,2	2080		57	75,2	23,7		10		
4	19,7	0,33	10,5	18	0,30	74,2	2180		60	81,4	25,0		10		
5	29,8	0,50	11,25	30	0,50	81,8	2750		61	92,9	28,8		9		
6	39,2	0,67	12,2	40,8	0,68	83,1	2875		65	94,7	29,6		10		
7	49,9	0,83	13,4	51,6	0,86	84,1	3135		65	107,2	33,2		10		
8	60,4	1,01	15,0	64,2	1,07	86,4	3665		64	122,9	38,7		11		
9	89,7	1,50	20,75	95,4	1,59	86,5	4730		63	171,5	54,1		15		
10	112,9	1,88	26,4	118,2	1,97	85,1	5740		65	213,2	69,4		17		

Table: D.1

Date: 2-5-'84

Measurements on CWD 145 with SCL III b

Stroke Vol: $0,92 \cdot 10^{-3}$ m³

Stroke: 0,06 m

Head: 4,8 m

Measur. nr: XIII

	n (rpm)	n (rps)		$\bar{\Phi}$ $\times 10^{-2}$ m³/m	$\bar{\Phi}$ $\times 10^{-3}$ m³/s	η_{vol} (%)	F_{max} (N)		$\eta_{mech.}$ (%)	Q_{max} (Nm)	$\bar{Q}$ (Nm)		α_{cl} (deg.)	α_{scl} meas.	α_{scl} theor.	Comments.
1	9,0	0,15		0	0	0	320		-	6,9	3,0		6	-	-	SCL. - open
2	13,4	0,22		0	0	0	500		-	12,1	4,2		8	-	90	SCL - open
3	14,5	0,24		6	0,10	45	1200		40	28,3	7,7		9	90	73	SCL. - closed
4	19,9	0,33		12,6	0,21	69	1300		47	35,2	10,2		9	61	44	"
5	30,2	0,50		21	0,35	76	1500		48	36,6	10,9		12	46	27	"
6	40,6	0,68		28,8	0,48	77	1500		49	36,0	10,8		11	42	20	"
7	50,0	0,83		36,6	0,61	80	1500		51	35,8	10,9		13	41	16	"
8	60,4	1,01		44,4	0,74	80	1550		48	38,9	11,5		14	42	13	"
9	93,0	1,55		69	1,15	81	1750		39	49,3	14,2		15	50	8	F_{max} = Slack force "
10	121,2	2,02		91,2	1,52	82	1970		33	63,8	17,4		15	57	7	F_{max} = Slack force "

Table: D 2

Date: 26-4-'84

Measurements on CND 145 with no leakhole

Stroke Vol: $0{,}28 \cdot 10^{-3}$ m³

Stroke: 0,06 m

Head: 4,2 m

Measur. nr: KII

	n (rpm)	n (rps)		$K10^{-3}$ Φ (m³/m)	$K10^{-3}$ $\bar{\Phi}$ (m³/s)	η_{vol} (%)	F_{max} (N)		$\eta_{mech.}$ (%)	Q_{max} (Nm)	$\bar{Q}$ (Nm)		α_{cl} (deg.)			Comments.
1	10,3	0,17		10,2	0,17	100	1200		68	32,8	10,3		9			
2	14,7	0,25		13,2	0,22	100	1220		66	33,0	10,6		11			
3	19,7	0,33		13,2	0,32	100	1390		56	28,5	12,4		9			
4	30,3	0,51		27,6	0,46	100	1630		56	41,2	18,4		11			
5	39,8	0,66		37,2	0,62	100	1620		61	39,6	16,5		12			
6	50,0	0,83		44,4	0,74	97	1620		58	39,3	11,8		11			
7	53,9	1,00		52,8	0,88	96	1670		53	43,9	12,6		12			
8	90,3	1,51		79,4	1,29	93	1995		43	49,7	15,3		14			F_{max} = Shock force
9	120,1	2,00		101,4	1,63	92	2370		35	65,0	18,6		17			F_{max} = Shock force.

Table: D·3

Date: 1-5-'84

Measurements on CWD 145 with 2 leakholes ⌀ 3 mm

Stroke Vol: $0{,}92 \cdot 10^{-3}$ m³

Stroke: 0,06 m

Head: 5 m

Measur. nr: X

	n (rpm)	n (rps)		Φ ($\times 10^{-3}$) (m^3/m)	Φ ($\times 10^{-2}$) (m^3/s)	η_{vol} (%)	F_{max} (N)		$\eta_{mech.}$ (%)	Q_{max} (Nm)	$\bar{Q}$ (Nm)		α_{ol} (deg)			Comments.
1	10,0	0,17		6,6	0,11	72	1130		52	30,5	9,2		9			
2	15,0	0,25		11,4	0,19	83	1800		57	32,0	10,5		12			
3	19,6	0,33		16,2	0,27	90	1340		54	36,6	12,1		9			
4	30,0	0,50		24	0,40	87	1600		49	49,0	12,8		11			
5	39,7	0,66		34,2	0,57	94	1580		55	49,0	12,3		10			
6	49,3	0,82		40,2	0,67	82	1580		51	38,7	12,6		10			
7	60,7	1,01		49,2	0,82	88	1580		48	41,8	13,3		12			
8	90,1	1,50		72	1,20	87	1790		41	47,4	15,4		14			
9	120,4	2,01		96,6	1,61	87	2110		34	61,9	18,3		16			F_{max} = Shock force.

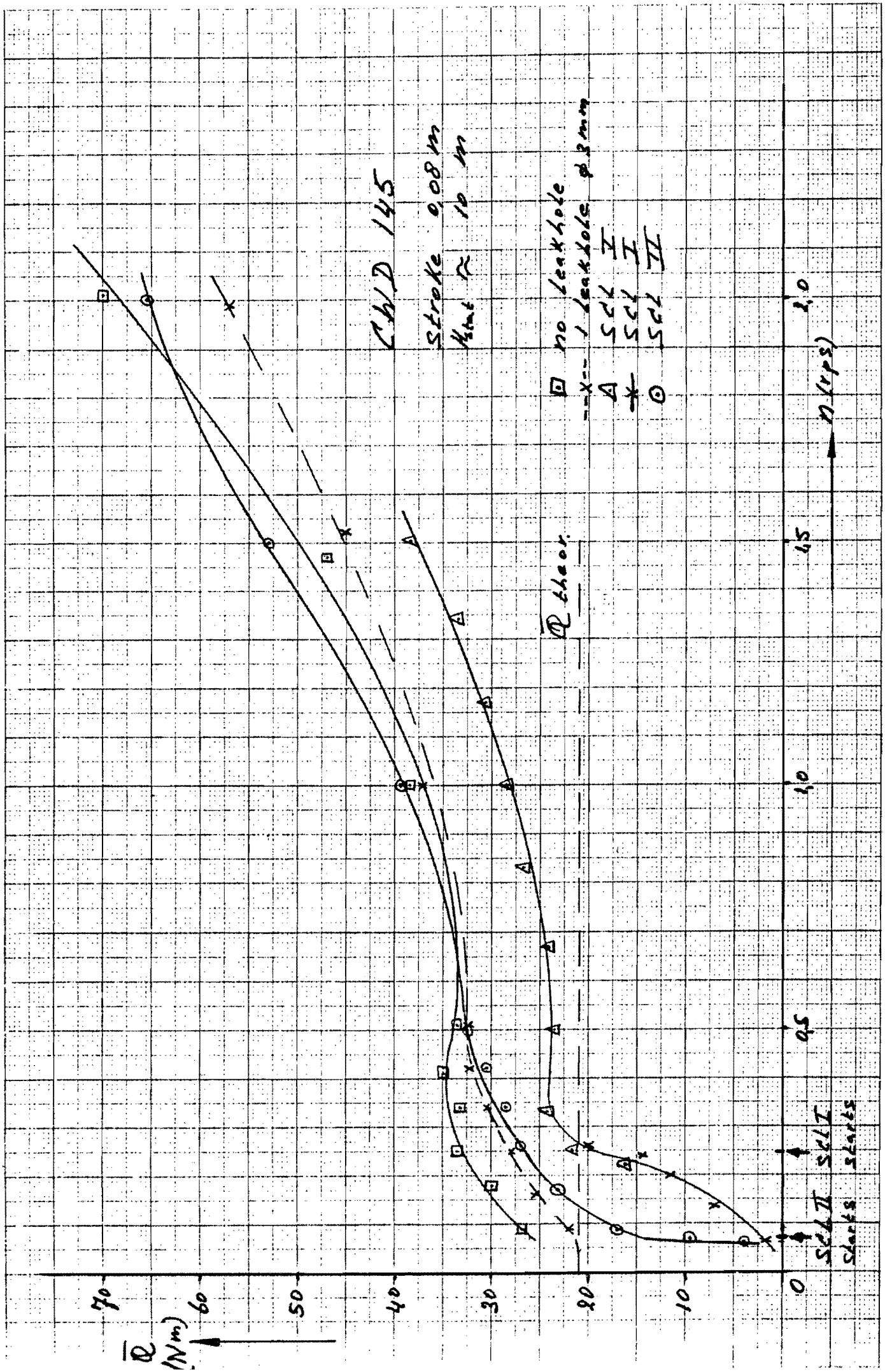
CHILD 145
Stroke 0,08 m
V_{tot} ≈ 10 m
□ no leakhole
--x-- 1 leakhole ϕ 3mm
Δ SCU II
+ SCU I
○ SCU III
$\bar{Q}$ theor.
$\bar{Q}$ (Nm)
n (rps)
SCU II starts
SCU I starts

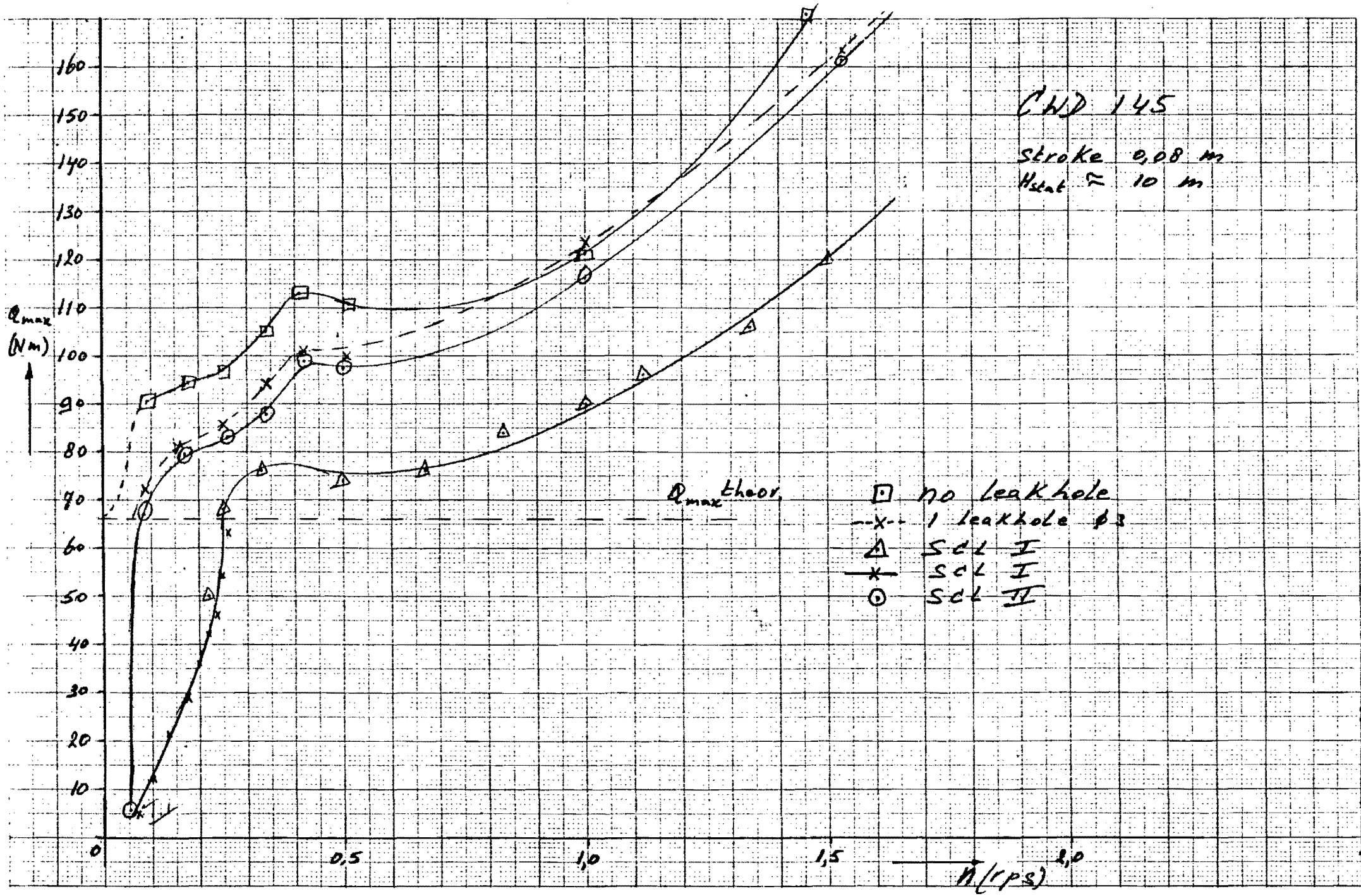
CHD 145
stroke 0,08 m
Hstat ≈ 10 m
Qmax (Nm)
Qmax theor.
no leakhole
1 leakhole ϕ2
Scl I
Scl I
Scl II
n (rps)
160
150
140
130
120
110
100
90
80
70
60
50
40
30
20
10
0
0,5
1,0
1,5
2,0

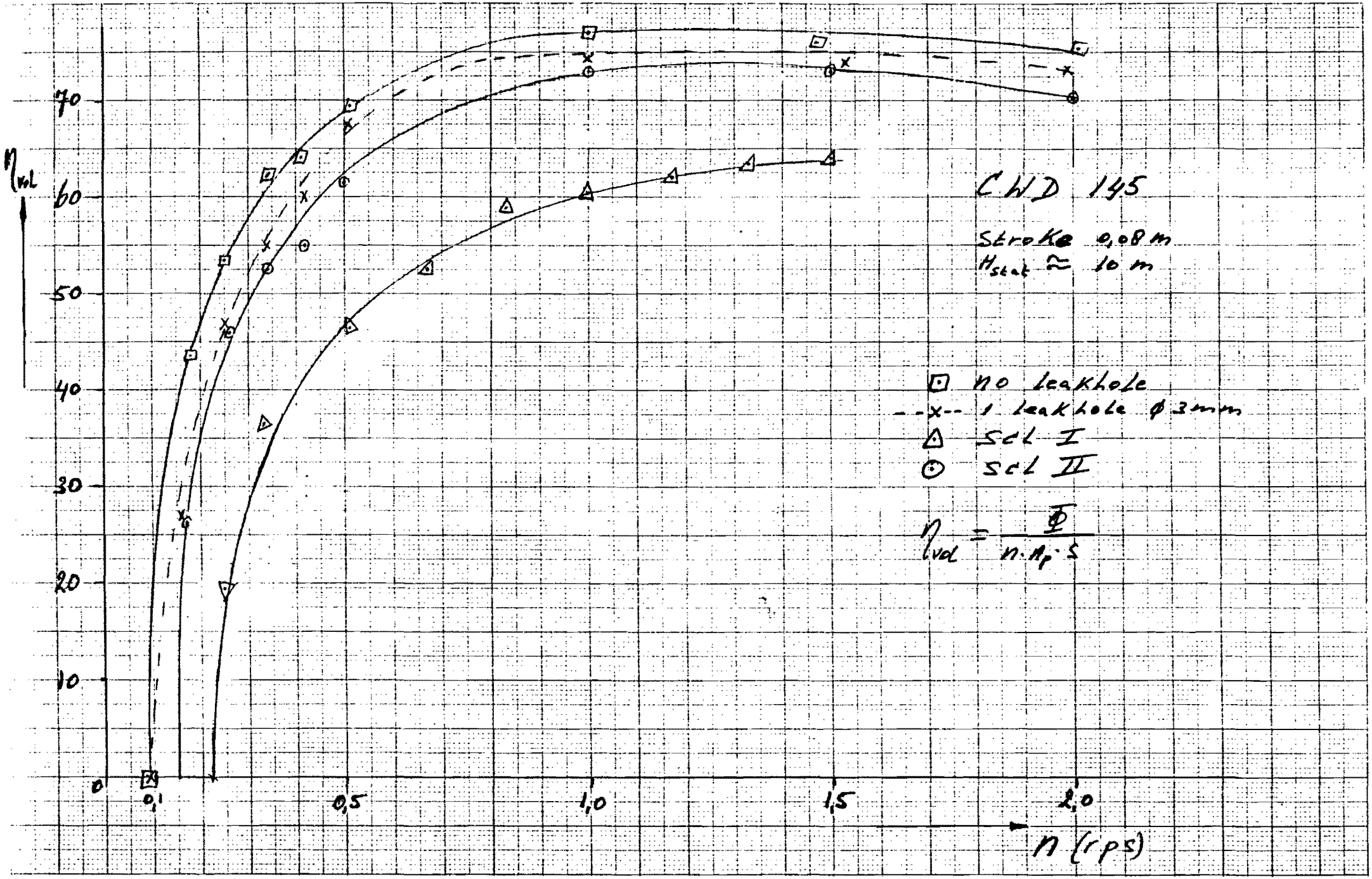
CWD 145
Stroke 0,08 m
$H_{stat} \simeq$ 10 m
no leakhole
1 leakhole ϕ 3mm
Scl I
Scl II
$\eta_{vol} = \frac{\Phi}{n \cdot A_p \cdot s}$
η_{vol}
70
60
50
40
30
20
10
0
0,1
0,5
1,0
1,5
2,0
n (rps)

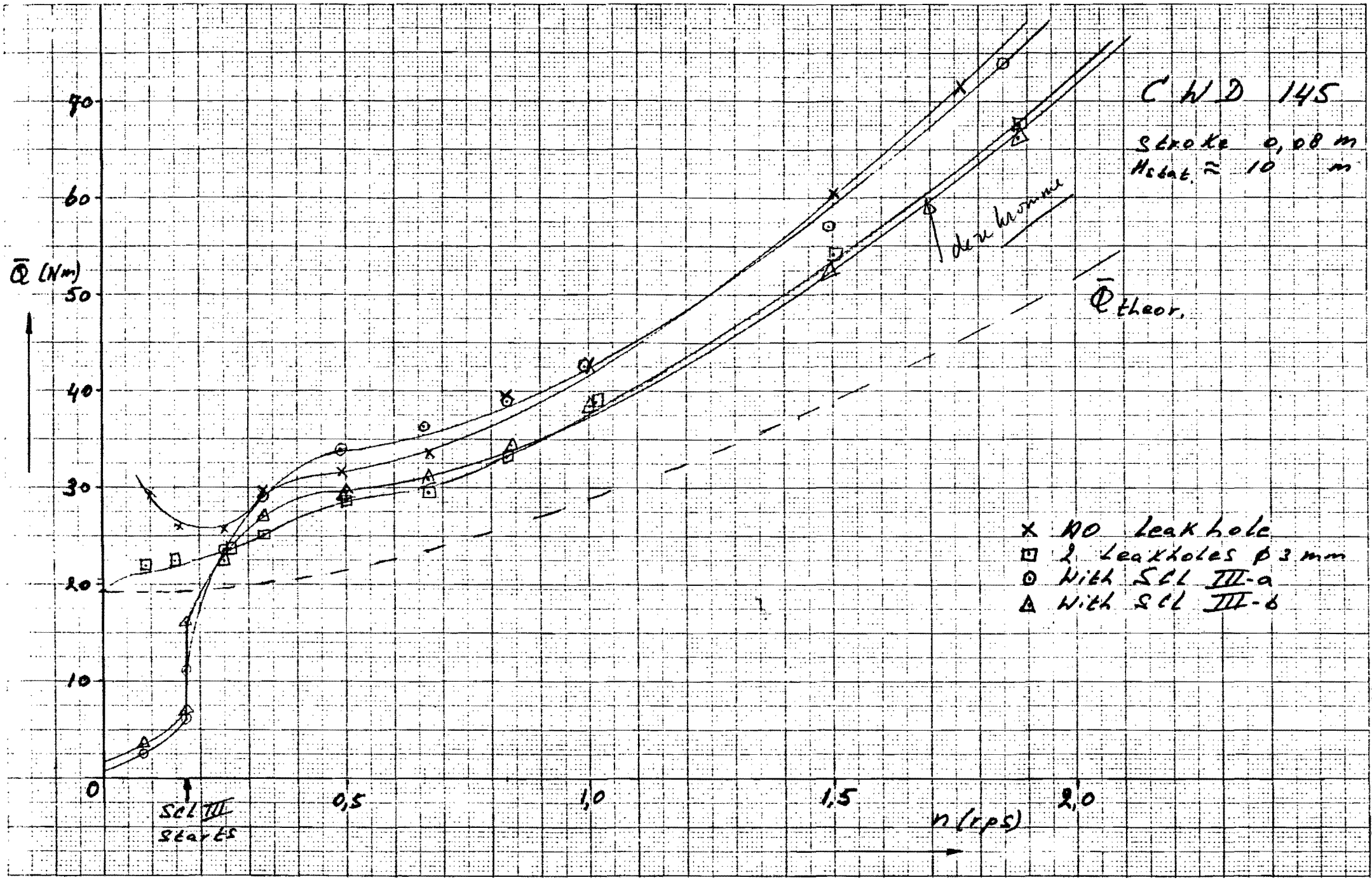
CWD 145
Stroke 0,08 m
Hstat. ≈ 10 m
Q̄ (Nm)
Q̄ theor.
n (rps)
0
10
20
30
40
50
60
70
0,5
1,0
1,5
2,0
Sct III
starts
× NO leak hole
□ 2 leakholes ϕ 3 mm
⊙ With Sct III-a
△ With Sct III-b

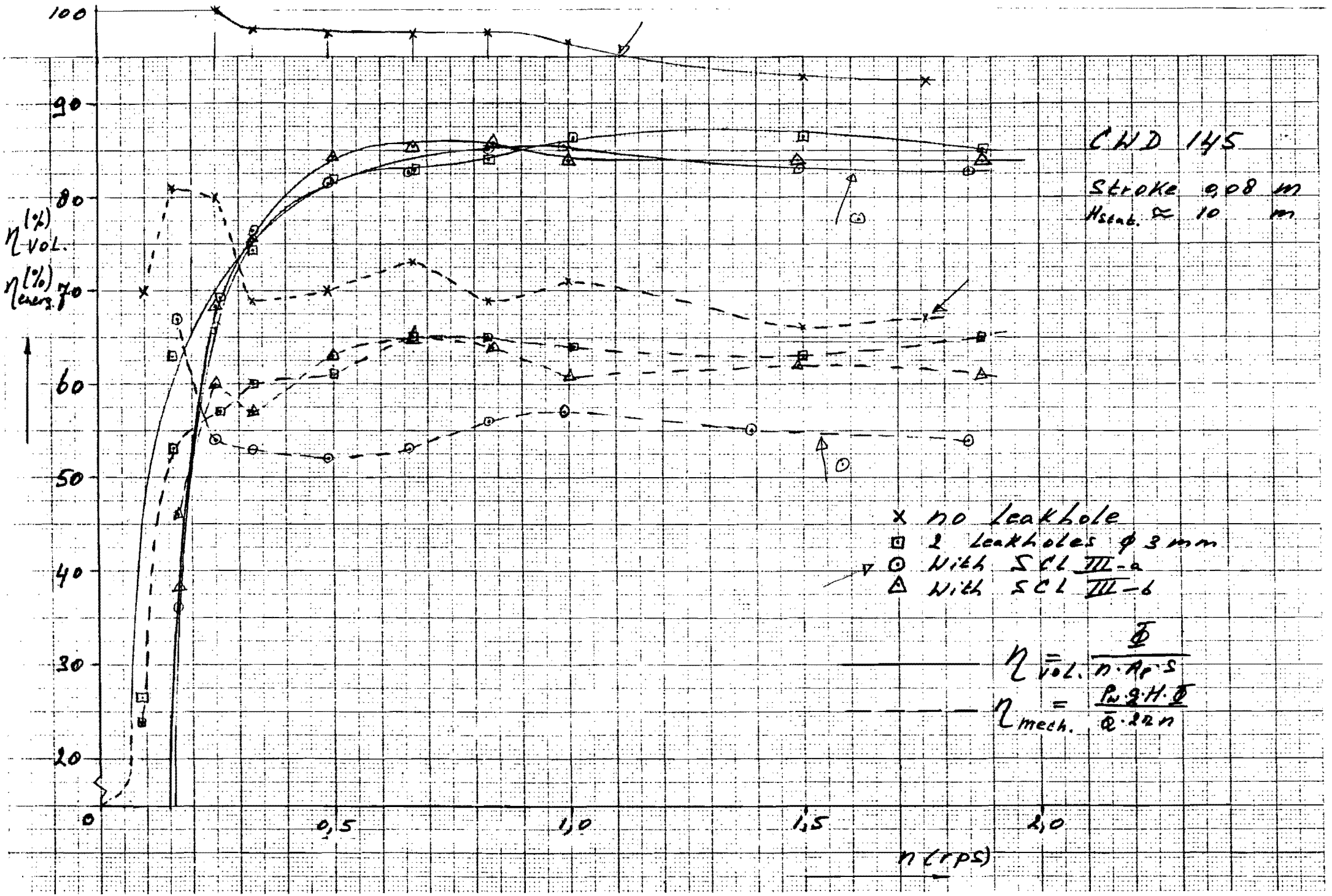
100
90
80
70
60
50
40
30
20
0
0,5
1,0
1,5
2,0
η (%) VOL.
η (%) MECH.
n (rps)
CWD 145
Stroke 9,08 m
Hstat. ≃ 10 m
× no Leakhole
□ 2 Leakholes ϕ 3 mm
○ With SCL III-a
△ With SCL III-b
η VOL. = Φ / n·Ap·s
η MECH. = Pw·g·H·Φ / Q·2πn

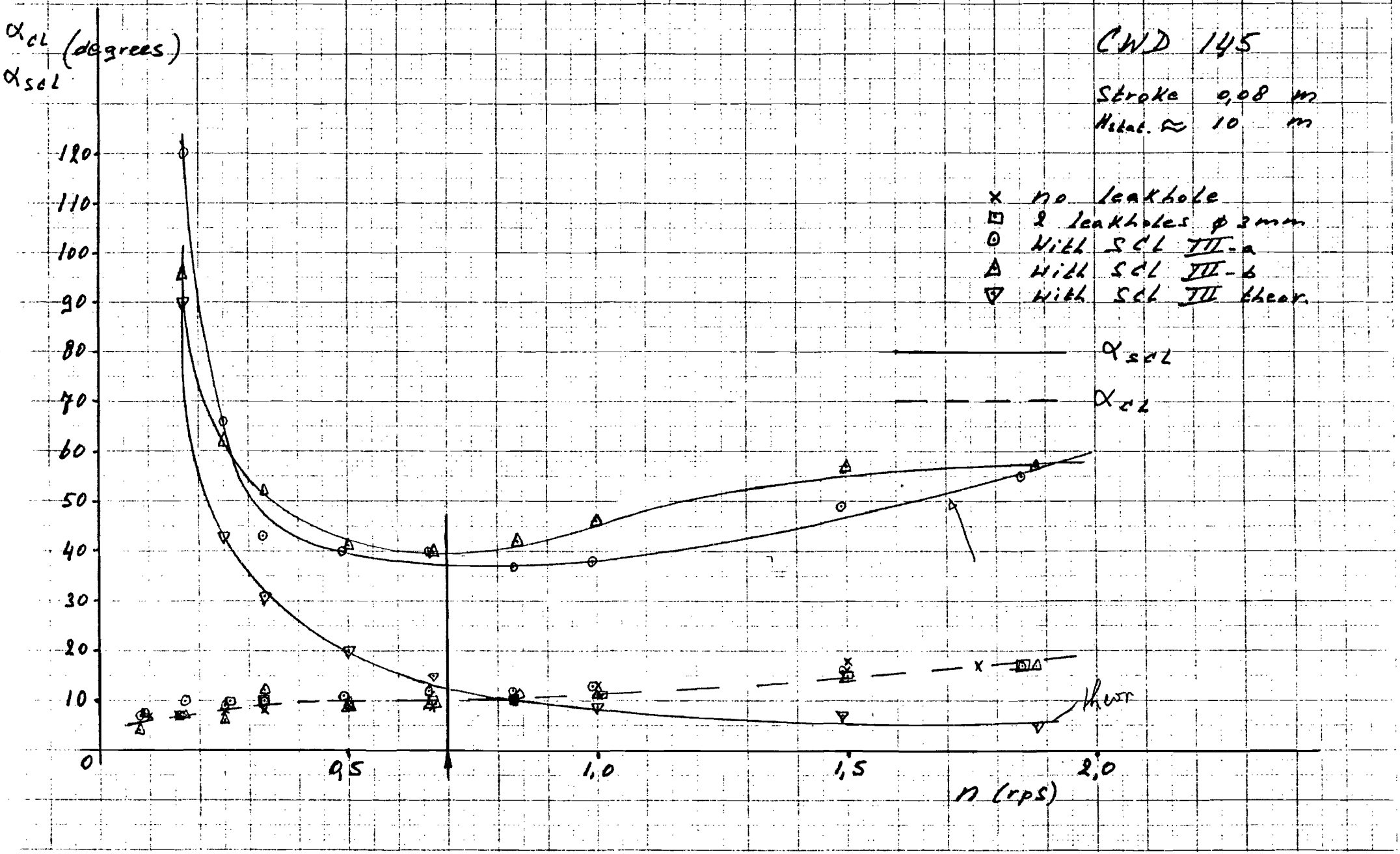
α_{cl} (degrees)
α_{scl}
CWD 145
Stroke 0,08 m
Hstat. ≈ 10 m
× no leakhole
□ 2 leakholes ϕ 3 mm
○ With SCL III-a
△ With SCL III-b
▽ With SCL III theor.
α_{scl}
α_{cl}
theor
120
110
100
90
80
70
60
50
40
30
20
10
0
9,5
1,0
1,5
2,0
n (rps)

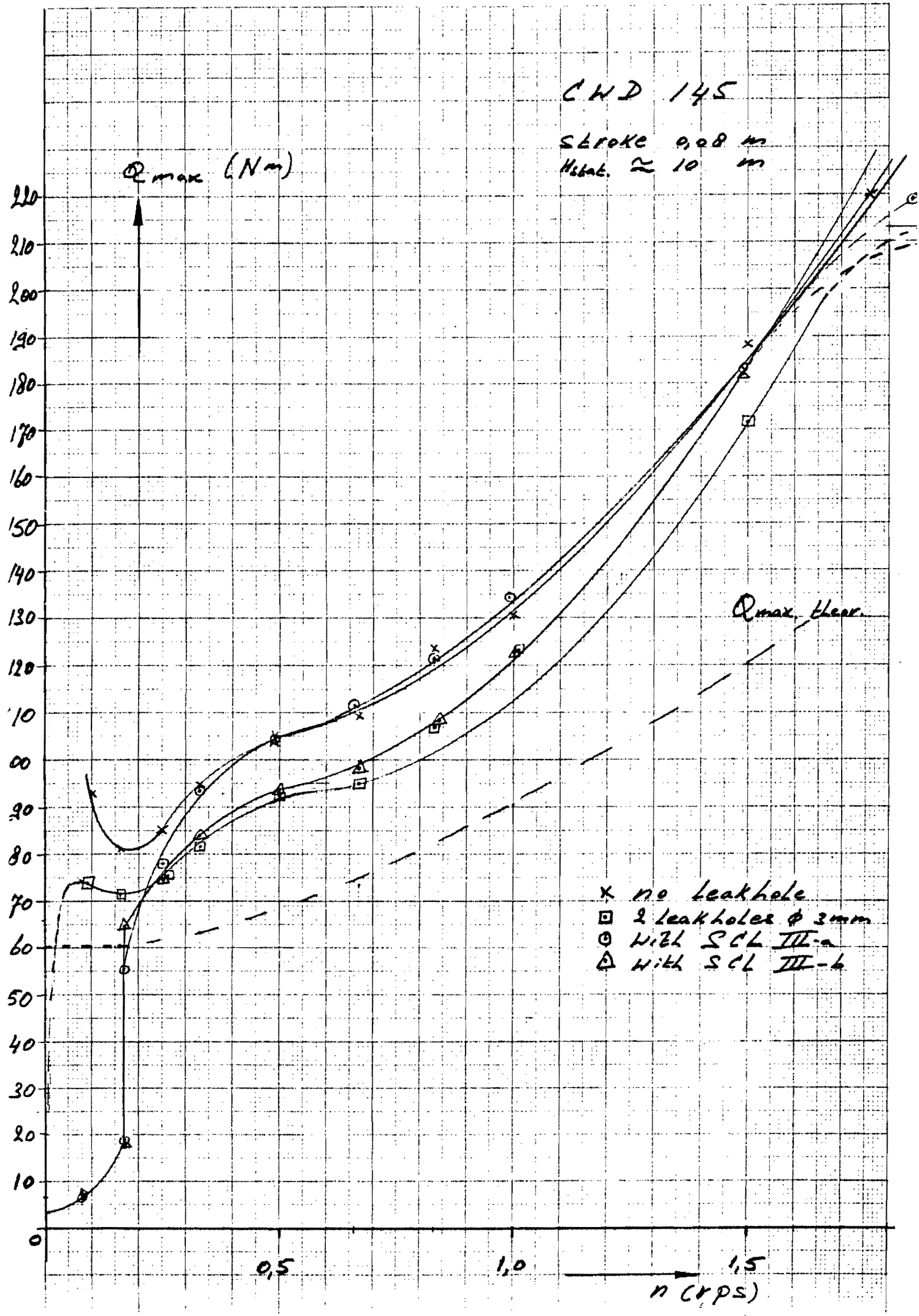
CWD 145
Stroke 0,08 m
Hstat. ≈ 10 m
Qmax (Nm)
Qmax. theor.
220
210
200
190
180
170
160
150
140
130
120
110
100
90
80
70
60
50
40
30
20
10
0
0,5
1,0
1,5
n (rps)
× no leakhole
□ 2 leakholes ϕ 3 mm
○ with SCL III-a
△ with SCL III-b

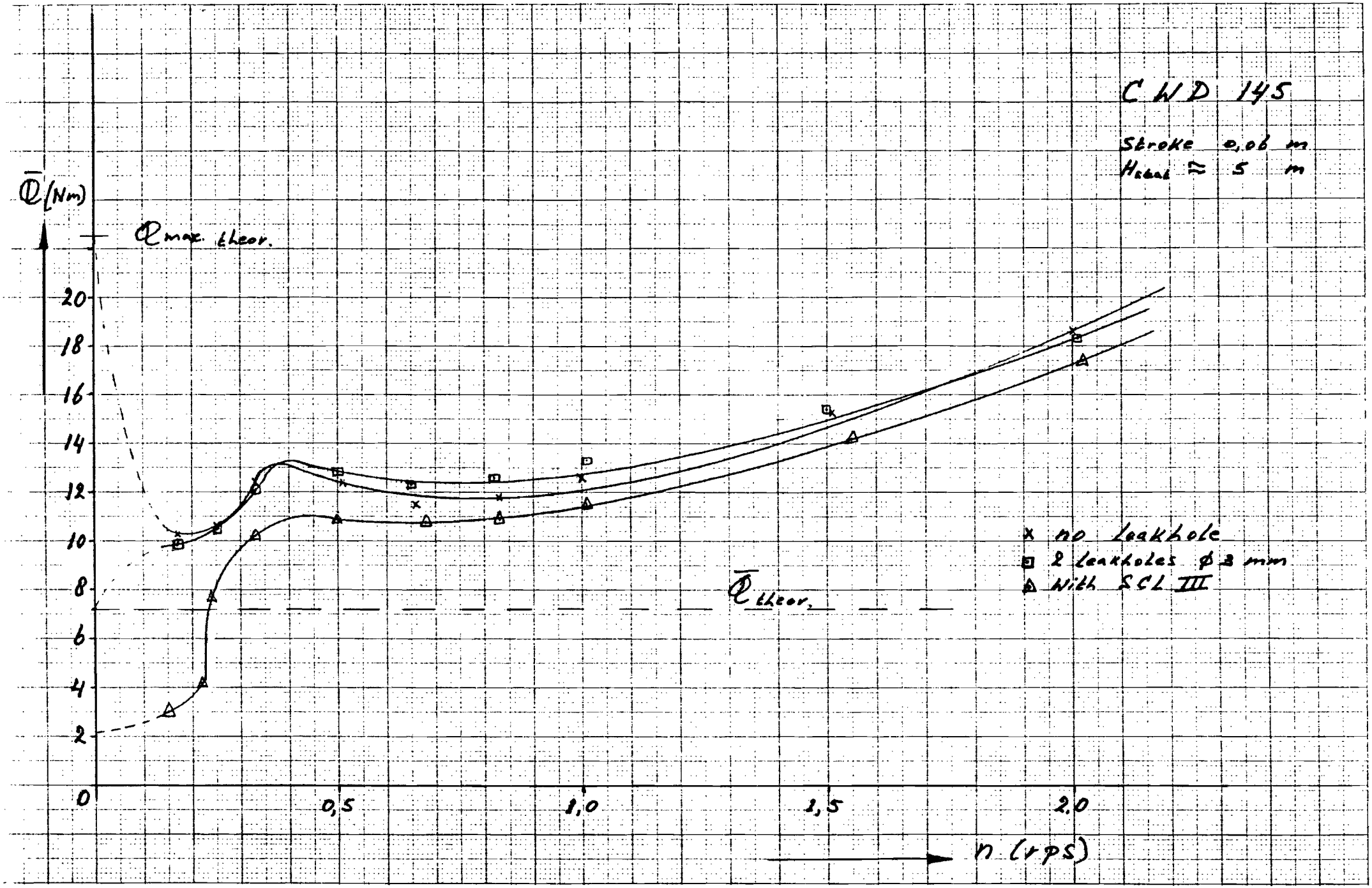
CWD 145
Stroke 0,06 m
Head ≈ 5 m
Q (Nm)
Q max. theor.
20
18
16
14
12
10
8
6
4
2
0
Q theor.
no leakhole
2 leakholes ϕ 3 mm
With SCL III
0,5
1,0
1,5
2,0
n (rps)

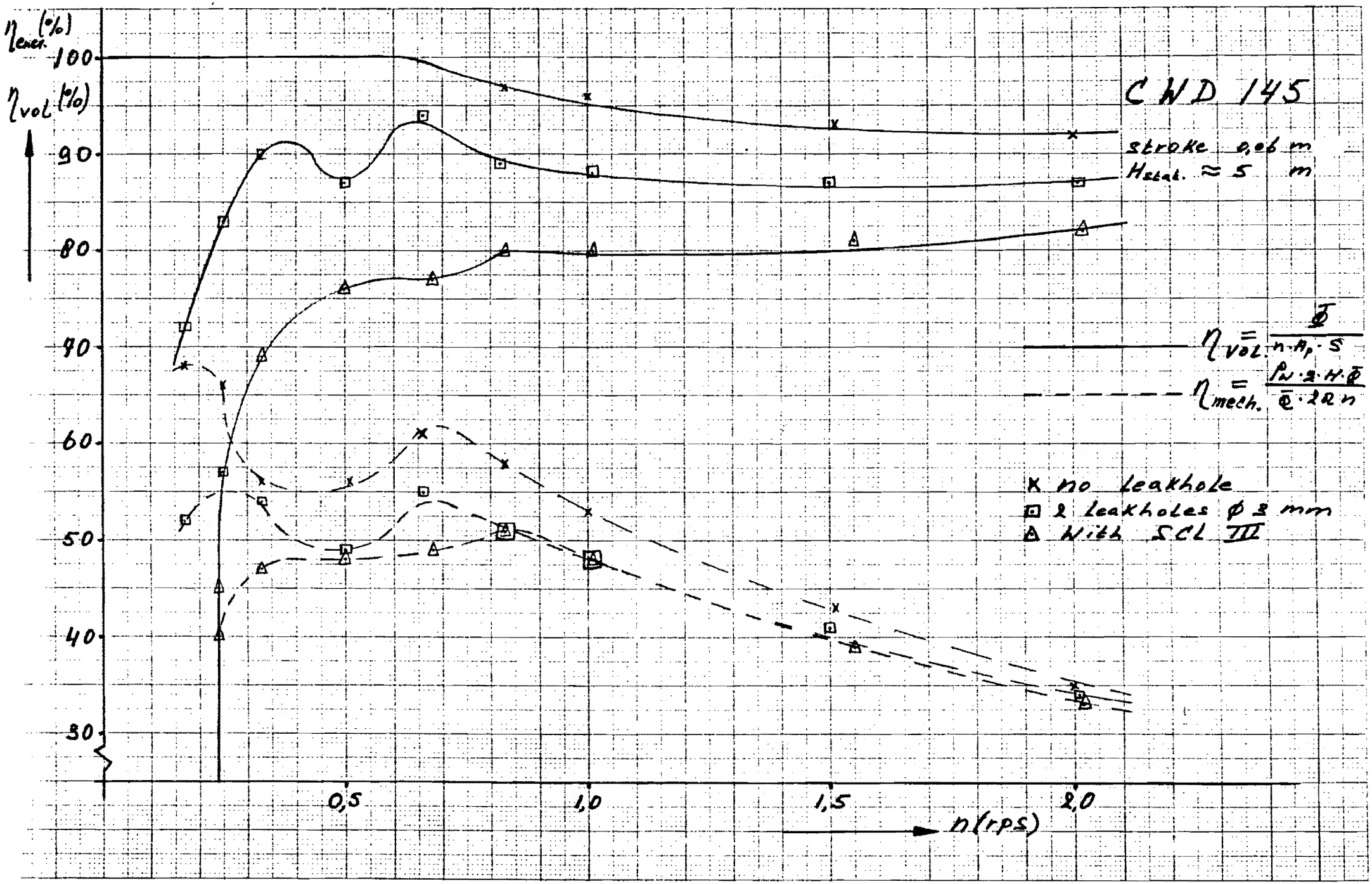
$\eta_{mech.}$ (%)
η_{vol} (%)
100
90
80
70
60
50
40
30
0,5
1,0
1,5
2,0
n (rps)
CWD 145
stroke 0,06 m
Head. ≈ 5 m
$\eta_{vol.} = \frac{Q}{n \cdot A_p \cdot s}$
$\eta_{mech.} = \frac{P_N \cdot 2 \cdot H \cdot Q}{\bar{Q} \cdot 2\pi n}$
× no leakhole
□ 2 leakholes ϕ 3 mm
△ With SCL III

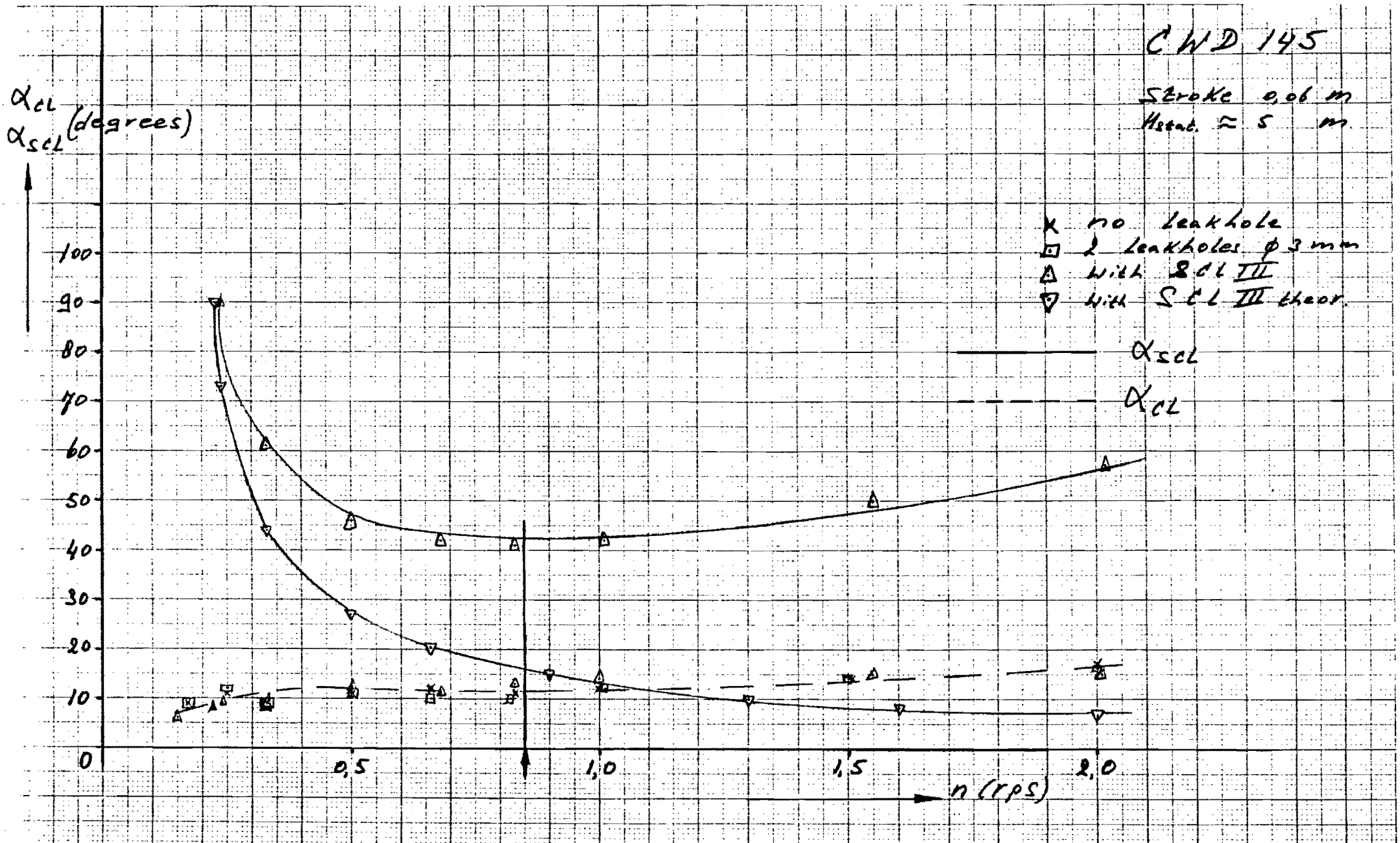
CWD 145
Stroke 0,06 m
Hstat. ≈ 5 m
× no leakhole
□ 2 leakholes ϕ 3 mm
△ with Scl III
▽ with Scl III theor.
αscl
αcl
αcl
αscl (degrees)
100
90
80
70
60
50
40
30
20
10
0
0,5
1,0
1,5
2,0
n (rps)


CWD 145
stroke 0,06 m
Hstat ≈ 5 m
Qmax (Nm)
70
60
50
40
30
20
10
0
0,5
1,0
1,5
2,0
n (rps)
Qmax. theor.
x no leakhole
⊡ 2 leakholes ϕ 3 mm
△ with SCL III b

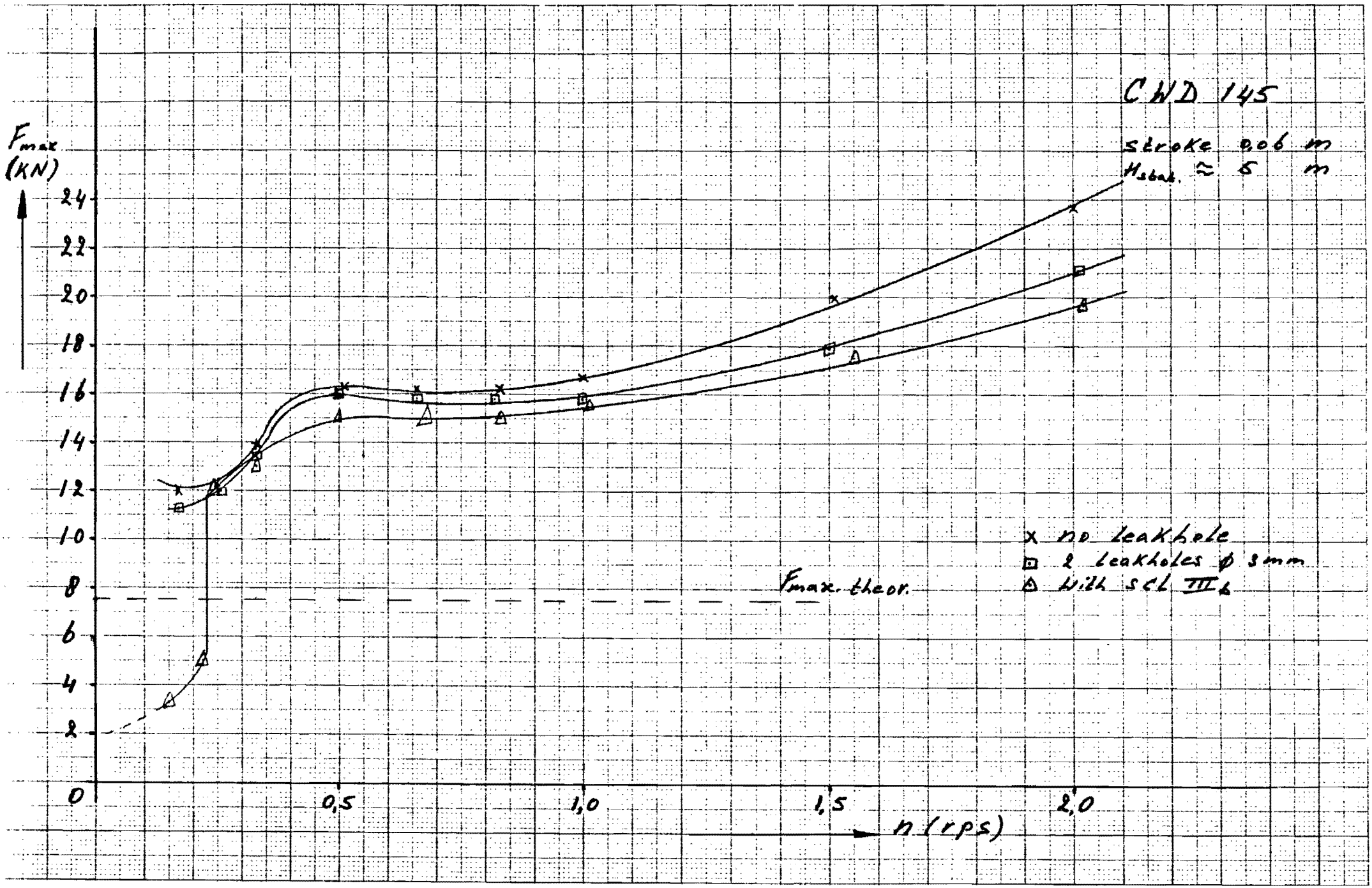
CWD 145
stroke 0,06 m
$H_{stat.} \simeq 5$ m
F_{max} (KN)
24
22
20
18
16
14
12
10
8
6
4
2
0
0,5
1,0
1,5
2,0
n (rps)
$F_{max.theor.}$
× no leakhole
□ 2 leakholes ϕ 3 mm
△ with SCL III b

and the corresponding velocity is

$$\mathbf{v} = -A\mathbf{u} + Br^2[\mathbf{n}(\mathbf{u}\cdot\mathbf{n}) - 2\mathbf{u}].$$

At the surface of the sphere† the following conditions must be satisfied. The normal velocity components outside (v_e) and inside (v_i) the drop must be zero:

$$v_{i,r} = v_{e,r} = 0.$$

The tangential velocity component must be continuous:

$$v_{i,\theta} = v_{e,\theta},$$

as must be the component $\sigma_{r\theta}$ of the stress tensor:

$$\sigma_{i,r\theta} = \sigma_{e,r\theta}.$$

The condition that the stress tensor components σ_{rr} are equal need not be written down; it would determine the required velocity u, which is more simply found in the manner shown below. From the above four conditions we obtain four equations for the constants a, b, A, B, whose solutions are

$$a = R\frac{2\eta+3\eta'}{4(\eta+\eta')}, \qquad b = R^3\frac{\eta'}{4(\eta+\eta')}, \qquad A = -BR^2 = \frac{\eta}{2(\eta+\eta')}.$$

By (20.14a), we have for the drag

$$F = 2\pi u\eta R(2\eta+3\eta')/(\eta+\eta').$$

As $\eta' \to \infty$ (corresponding to a solid sphere) this formula becomes Stokes' formula. In the limit $\eta' \to 0$ (corresponding to a gas bubble) we have $F = 4\pi u\eta R$, i.e. the drag is two-thirds of that on a solid sphere.

Equating F to the force of gravity on the drop, $\frac{4}{3}\pi R^3(\rho-\rho')g$, we find

$$u = \frac{2R^2g(\rho-\rho')(\eta+\eta')}{3\eta(2\eta+3\eta')}.$$

PROBLEM 3. Two parallel plane circular disks (of radius R) lie one above the other a small distance apart; the space between them is filled with fluid. The disks approach at a constant velocity u, displacing the fluid. Determine the resistance to their motion (O. REYNOLDS).

SOLUTION. We take cylindrical co-ordinates, with the origin at the centre of the lower disk, which we suppose fixed. The flow is axisymmetric and, since the fluid layer is thin, predominantly radial: $v_z \ll v_r$, and also $\partial v_r/\partial r \ll \partial v_r/\partial z$. Hence the equations of motion become

$$\eta\frac{\partial^2 v_r}{\partial z^2} = \frac{\partial p}{\partial r}, \qquad \frac{\partial p}{\partial z} = 0, \tag{1}$$

$$\frac{1}{r}\frac{\partial(rv_r)}{\partial r} + \frac{\partial v_z}{\partial z} = 0, \tag{2}$$

† We may neglect the change of shape of the drop in its motion, since this change is of a higher order of smallness. However, it must be borne in mind that, in order that the moving drop should in fact be spherical, the forces due to surface tension at its boundary must exceed the forces due to pressure differences, which tend to make the drop non-spherical. This means that we must have $\eta u/R \ll \alpha/R$, where α is the surface-tension coefficient, or, substituting $u \sim R^2g\rho/\eta$,

$$R \ll \sqrt{(\alpha/\rho g)}.$$

with the boundary conditions

$$\text{at } z = 0: \qquad v_r = v_z = 0;$$
$$\text{at } z = h: \qquad v_r = 0, \quad v_z = -u;$$
$$\text{at } r = R: \qquad p = p_0,$$

where h is the distance between the disks, and p_0 the external pressure. From equations (1) we find

$$v_r = \frac{1}{2\eta}\frac{\partial p}{\partial r} z(z-h).$$

Integrating equation (2) with respect to z, we obtain

$$u = \frac{1}{r}\frac{\mathrm{d}}{\mathrm{d}r}\int_0^h r v_r \,\mathrm{d}z = -\frac{h^3}{12\eta r}\frac{\mathrm{d}}{\mathrm{d}r}\left(r\frac{\mathrm{d}p}{\mathrm{d}r}\right),$$

whence

$$p = p_0 + \frac{3\eta u}{h^3}(R^2 - r^2).$$

The total resistance to the moving disk is

$$\boxed{F = 3\pi\eta u R^4/2h^3.}$$

§21. The laminar wake

In steady flow of a viscous fluid past a solid body, the flow at great distances behind the body has certain characteristics which can be investigated independently of the particular shape of the body.

Let us denote by **U** the constant velocity of the incident current; we take the direction of **U** as the x-axis, with the origin somewhere inside the body. The actual fluid velocity at any point may be written $\mathbf{U}+\mathbf{v}$; $\mathbf{v}$ vanishes at infinity.

It is found that, at great distances behind the body, the velocity $\mathbf{v}$ is noticeably different from zero only in a relatively narrow region near the x-axis. This region, called the *laminar wake*,† is reached by fluid particles which move along streamlines passing fairly close to the body. Hence the flow in the wake is essentially rotational. On the other hand, the viscosity has almost no effect at any point on streamlines that do not pass near the body, and the vorticity, which is zero in the incident current, remains practically zero on these streamlines, as it would in an ideal fluid. Thus the flow at great distances from the body may be regarded as potential flow everywhere except in the wake.

We shall now derive formulae relating the properties of the flow in the wake to the forces acting on the body. The total momentum transported by the fluid through any closed surface surrounding the body is equal to the

† In contradistinction to the turbulent wake; see §36.

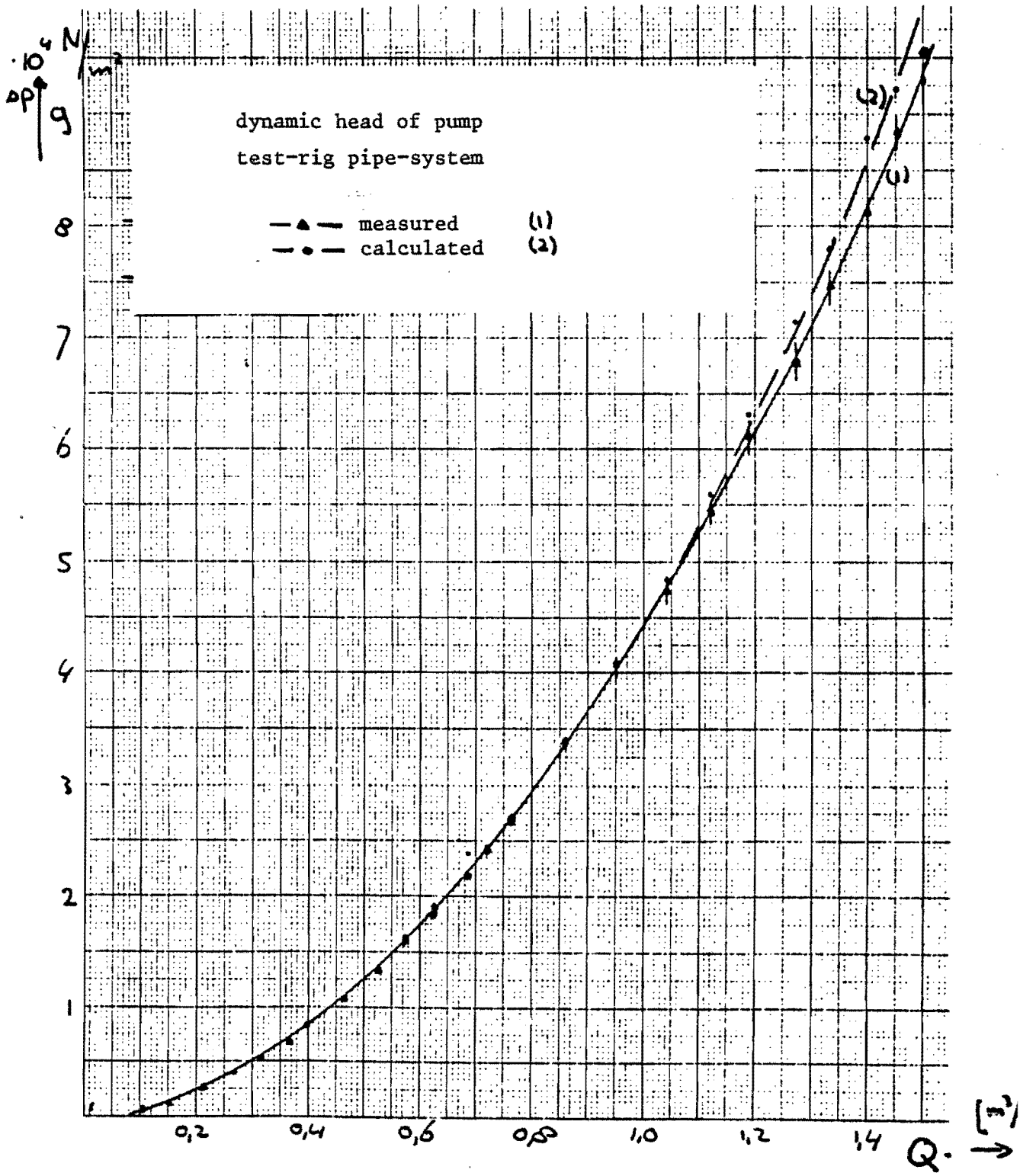

Measured by M. Hilbers